



NRL/MR/7320--15-9590

Validation Test Report for the Arctic Cap Nowcast/Forecast System as a Fractures/Leads and Polynyas Product

JULIA W. CROUT
Vencore Services and Solutions, Inc.
Reston, Virginia

PAMELA G. POSEY
Ocean Dynamics and Prediction Branch
Oceanography Division

May 26, 2015

Approved for public release; distribution is unlimited.

REPORT DOCUMENTATION PAGE

Form Approved
OMB No. 0704-0188

Public reporting burden for this collection of information is estimated to average 1 hour per response, including the time for reviewing instructions, searching existing data sources, gathering and maintaining the data needed, and completing and reviewing this collection of information. Send comments regarding this burden estimate or any other aspect of this collection of information, including suggestions for reducing this burden to Department of Defense, Washington Headquarters Services, Directorate for Information Operations and Reports (0704-0188), 1215 Jefferson Davis Highway, Suite 1204, Arlington, VA 22202-4302. Respondents should be aware that notwithstanding any other provision of law, no person shall be subject to any penalty for failing to comply with a collection of information if it does not display a currently valid OMB control number. **PLEASE DO NOT RETURN YOUR FORM TO THE ABOVE ADDRESS.**

1. REPORT DATE (DD-MM-YYYY) 26-05-2015			2. REPORT TYPE Memorandum Report			3. DATES COVERED (From - To)		
4. TITLE AND SUBTITLE Validation Test Report for the Arctic Cap Nowcast/Forecast System as a Fractures/Leads and Polynyas Product						5a. CONTRACT NUMBER		
						5b. GRANT NUMBER		
						5c. PROGRAM ELEMENT NUMBER 0603207N		
6. AUTHOR(S) Julia W. Crout* and Pamela G. Posey						5d. PROJECT NUMBER		
						5e. TASK NUMBER		
						5f. WORK UNIT NUMBER 73-9066-04-5		
7. PERFORMING ORGANIZATION NAME(S) AND ADDRESS(ES) Naval Research Laboratory Oceanography Division Stennis Space Center, MS 39529-5004						8. PERFORMING ORGANIZATION REPORT NUMBER NRL/MR/7320--15-9590		
9. SPONSORING / MONITORING AGENCY NAME(S) AND ADDRESS(ES) Space & Naval Warfare Systems Command 2451 Crystal Drive Arlington, VA 22245-5200						10. SPONSOR / MONITOR'S ACRONYM(S) SPAWAR		
						11. SPONSOR / MONITOR'S REPORT NUMBER(S)		
12. DISTRIBUTION / AVAILABILITY STATEMENT Approved for public release; distribution is unlimited.								
13. SUPPLEMENTARY NOTES *Vencore Services and Solutions, Inc., 11091 Sunset Hills Road, Suite 200, Reston, VA 20190.								
14. ABSTRACT This document serves as the Validation Test Report (VTR) for the Naval Research Laboratory (NRL) Arctic Cap Nowcast/Forecast System (ACNFS) ability to capture and predict sea ice areas of opening Fractures/Leads, And Polynyas (FLAP). ACNFS calculates motion rates (opening/closing, ridging, divergence, and shear) in addition to numerous other products such as ice concentration, ice thickness, and ice drift. A combination of these parameters is used to produce a product of opening rates that represent areas of FLAPs. This VTR documents a series of comparison studies performed using ACNFS strain rate fields and validates the opening rate products against an 11 month period of National Ice Center (NIC) FLAP messages from January through November 2012. Forecasted ACNFS fields are evaluated for the period of February through June 2014 on daily 24 hours through 7-day forecasts. Additional comparisons are shown for ICEX-2014. This validation assessment was performed using ACNFS with some limited comparisons with the Global Ocean Forecast System (GOFS 3.1). GOFS 3.1 uses the same ocean model coupling and sea ice model as ACNFS and is expected to perform similarly. Overall, ACNFS along with GOFS 3.1 provided a reasonable prediction of the openings not available elsewhere in both the nowcast and forecast mode and performed better than persistence.								
15. SUBJECT TERMS Sea ice forecasting system HYCOM Lead opening validation Lead opening CICE								
16. SECURITY CLASSIFICATION OF:				17. LIMITATION OF ABSTRACT	18. NUMBER OF PAGES	19a. NAME OF RESPONSIBLE PERSON Pamela G. Posey		
a. REPORT Unclassified Unlimited	b. ABSTRACT Unclassified Unlimited	c. THIS PAGE Unclassified Unlimited		Unclassified Unlimited	43	19b. TELEPHONE NUMBER (include area code) (228) 688-5596		

Table of Contents

1	Introduction	1
2	Descriptions	2
2.1	ACNFS Opening Rate	2
2.2	ACNFS Accumulated Openings	5
2.3	ACNFS Opening Rate Contours	7
3	Validation	8
3.1	Thresholds	9
3.2	Model Best Quality	10
3.2.1	FLAP Message Validation	10
3.2.2	RADARSAT Model Analysis	11
3.3	Forecasting	12
3.3.1	Reference Hindcasts	13
3.3.2	Persistence versus Model Forecast	22
3.3.3	U.S. Navy Arctic Submarine Laboratory Ice Exercise (ICEX)	23
3.4	Polynyas	30
3.5	Seasonal Variation	32
4	Summary and Recommendations	35
5	Acknowledgements	36
6	References	37
7	Acronyms	38

List of Figures

Figure 1: Top: Notional FLAP message for Arctic region north of Greenland Sea. Left: MODIS imagery with fracture poly-lines in green, polynya in magenta, and ice edge in red. Right: ACNFS opening rate valid for same time period.	1
Figure 2: Daily maximum (top) and mean (bottom) opening rate values.	3
Figure 3: Distribution of opening rate values. Cells with 0 opening rate are not included.	4
Figure 4: ACNFS opening rate for 00Z January 05, 2012. a) default scale, 0 – max scale. b) scale 0-15%/day. c) scale 0-4%/day.	4
Figure 5: April 20, 2012 ACNFS opening rate (left) and MODIS imagery (right) just off the northern coast of Greenland. ...	5
Figure 6: Equation 3 represented pictorially with basin wide openings for May 19, 2014 accumulating 3 previous days of weighted opening rates reduced by convergence rates.	6
Figure 7: Regional openings for March 19, 2014 accumulating 2 previous days of weighted opening rates reduced by convergence rates. Top right panel shows NPP VIIRS contrast satellite image valid March 18, 2014 (courtesy of NRL – Monterey).	7
Figure 8: Clockwise from left: VIIRS imagery of Chukchi Sea January 13, 2014 (Courtesy of NRL/Monterey); ACNFS opening rate for same date; ACNFS opening rate for same date with opening rate contour overlaid.	8
Figure 9: ACNFS opening rate plotted at different scales. Left: 0 to the maximum opening rate of 1510 %/day. Middle: 0 to 50 %/day. Top: 0 to 4 %/day.	9
Figure 10: ACNFS openings greater than different threshold values. Left: opening rate > 0.1 %/day. Middle: opening rate > 0.5 %/day. Top: opening rate > 1.0 %/day.	10
Figure 11: February 20 to February 26, 2008 deformation and velocity fields from RADARSAT processing system (left 6 panels - RADARSAT and the ACNFS model fields (right 6 panels).	12
Figure 12: Forecast and Reference opening rate plots from February 13, 2014 nowcast.	14
Figure 13: Forecast and Reference ice drift plots from February 13, 2014 nowcast.	15
Figure 14: Forecast and Reference opening rate plots from March 11, 2014 nowcast.	16
Figure 15: Forecast and Reference ice drift plots from March 11, 2014 nowcast.	17
Figure 16: Forecast and Reference opening rate plots from March 11, 2014 nowcast for Kara Sea.	18
Figure 17: Forecast and Reference air stress plots from March 11, 2014 nowcast for Kara Sea.	19
Figure 18: Root Mean Square Error of the opening rate forecasts. Forecast time periods are from February through June 2014.	20
Figure 19: Contingency plot threshold selection.	21
Figure 20: Daily and mean accuracy, sensitivity, and specificity of ACNFS model forecasts out to 7 days. (February through June 2014).	22
Figure 21: Persistence and model forecasts RMS Error in opening rate. (February through June 2014)	23
Figure 22: Daily and mean accuracy, sensitivity, and specificity of ACNFS model forecasts and ACNFS persistence out to 7 days. (February through June 2014)	23
Figure 23: Beaufort Sea ACNFS Air stress for March 14, 15, and 16, 2014. ICEX 2014 ice camp general region outlined in red.	24
Figure 24: Beaufort Sea MODIS and RADARSAT-2 mosaic image for March 16, 2014.	25
Figure 25: Beaufort Sea ACNFS Opening rate nowcast and forecasts for March 16, 2014.	26
Figure 26: Beaufort Sea ACNFS Ice velocity 6-day out forecast for March 20, 2014.	27
Figure 27: Beaufort Sea ACNFS Opening rate hindcast, nowcast, and 24-hour forecast.	28
Figure 28: Beaufort Sea MODIS mosaic image for March 22, 2014. Wind and ice drift vectors overlaid.	29
Figure 29: Open ocean polynya August 16, 2012. Right: MODIS imagery (NASA, 2014) with ACNFS 40% concentration contour overlaid in black. Top, left: ACNFS opening rate with 40% concentration contour. Bottom, left: ACNFS ice concentration.	30
Figure 30: VIIRS Near-Constant Contrast (NCC) imagery (NRL-MRY, 2014) over Kara Sea from April 15 through April 22, 2014.	31
Figure 31: ACNFS Opening rate with 70% ice concentration contour in black for Kara Sea from April 15 through April 22, 2014.	31
Figure 32: RMS Error of the opening rate forecasts. Winter months are shown in shades of blue. Spring months are shown in shades of green.	32
Figure 33: Specificity, Sensitivity, and Accuracy classification errors of opening rate forecasts. Winter months are shown in shades of blue. Spring months are shown in shades of green.	33
Figure 34: Daily number of ice cells with concentration greater than 15%.	33

List of Tables

Table 1: FLAP area prediction comparison categories totals “√” indicated a strong match; “?” indicates a match to some degree, and “✘” indicates a poor match	11
Table 2: Contingency table used for forecasting ice openings.	21
Table 3: FLAP area prediction comparison categories totals broken out by season.	34
Table 4: FLAP area skill totals.	35
Table 5: Flap area forecast skill metrics for first 72 hours.	35

1 Introduction

The Naval Research Laboratory (NRL) Arctic Cap Nowcast/Forecast System (ACNFS) provides nowcast and forecast fields of ice parameters such as ice concentration, ice thickness, and ice drift which have been validated using observational data sets (Posey et al., 2010). ACNFS also provides ice motion strain rate fields of divergence, shear, and opening rate which can be used to provide an indication of zones of ice fracturing of leads and polynyas.

The National Ice Center (NIC) produces a Fractures/Leads and Polynyas (FLAP) product which is a formatted text message that identifies navigation and surfaceable features in the ice over large areas. The messages contains the latitude/longitude pairs delineating FLAPs, as well as remarks on the orientation, and ice types that a NIC ice analyst generated from available imagery. FLAP messages are produced for non-routine, special operations and exercises (submarine and surface ships) disseminated via message traffic and Submarine Forces broadcast. Figure 1 shows a notional example of a FLAP message built from Moderate Resolution Imaging Spectroradiometer (MODIS) imagery and the corresponding ACNFS opening rate product.

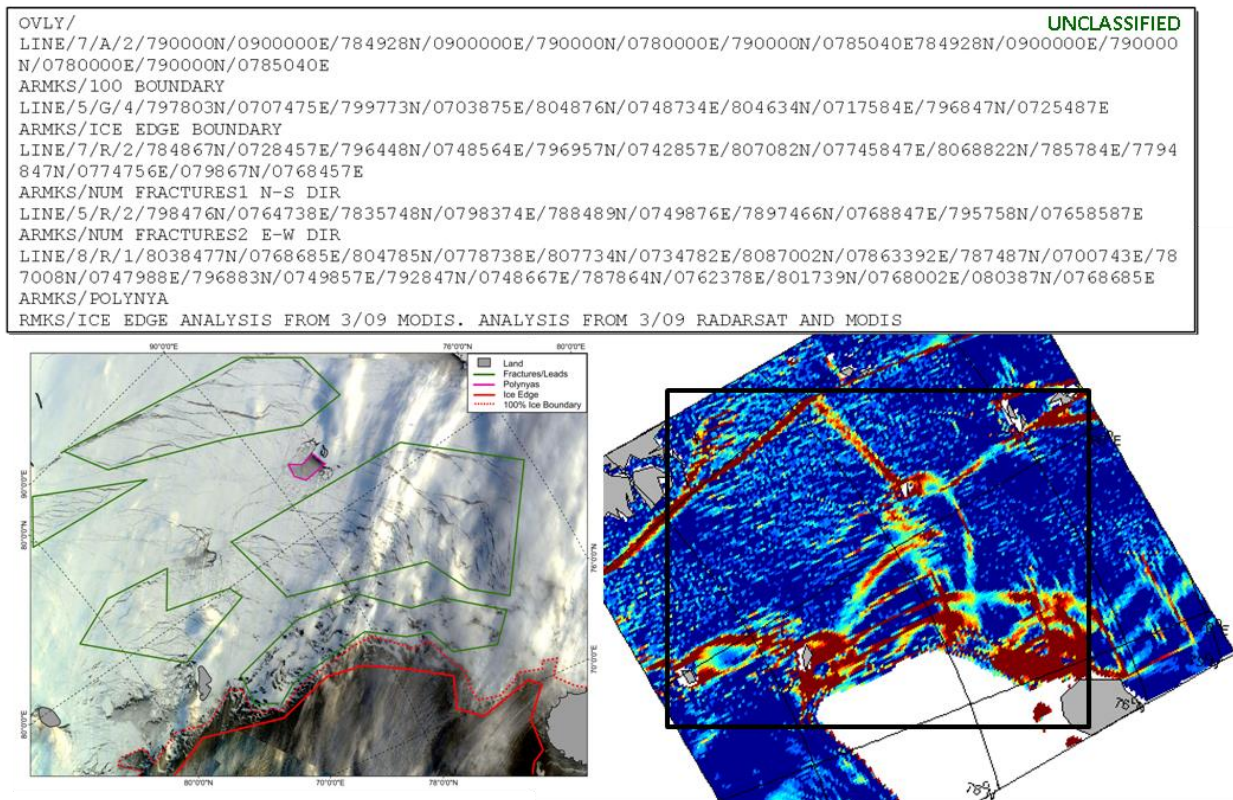


Figure 1: Top: Notional FLAP message for Arctic region north of Kara Sea. Left: MODIS imagery with fracture poly-lines in green, polynya in magenta, and ice edge in red. Right: ACNFS opening rate valid for same time period.

As part of the NIC Operational Evaluation (OPEVAL) of ACNFS (Helfrich, 2012), the NIC's Operations Department (OPS, N3) performed a utilization study of ACNFS beyond its objective testing of ice concentration, thickness and drifts to compare ACNFS lead opening rate to the

daily NIC analysis. The ACNFS opening rate was rated showing “good” potential for ice charting and as “very good” potential for FLAP and annotated imagery special support generation. The NIC limited comparisons showed that the ACNFS provided a general understanding for regional potential formation of leads, but was less able to resolve actual location and orientation. Also noted in the NIC OPS evaluation was the importance in forecasting lead openings.

Initial comparisons of ACNFS and MODIS imagery studies by NRL were similar to NIC findings in their OPEVAL testing. Whereas the scale of the imagery was between 250 m and 1 km and often a mosaic of imagery; the scale of ACNFS is approximately 3.5 km. While the ACNFS opening rate products looked realistic, they rarely matched the fracture-to-fractures details in the satellite imagery. Given the dynamic nature, temporal and spatial scales, and the model ice rheology, individual fracture of opening grid cells are not expected to be resolved. The model did well depicting relative regions of fractures which are similar to the FLAP areas identified by the NIC FLAP messages. As shown in Section 3.2.1 the model does well capturing the fracture field on this scale.

This Validation Test Report documents a series of comparison studies performed using ACNFS strain rate fields – in particular, the opening rate and openings based on an accumulation of opening fields. ACNFS opening rate products were validated against an 11 month period of FLAP messages from January through November 2012. The FLAP messages provided reference data to validate the best quality two-day hindcast ACNFS model output. Forecasted ACNFS fields are also evaluated for the period of February through June 2014 on daily 24 hour through 168 hour forecasts.

2 Descriptions

2.1 ACNFS Opening Rate

The ACNFS (Posey et al. , 2010) consists of the Los Alamos Sea Ice Model, the Community Ice Code (CICE) (Hunke and Lipscomb, 2004) coupled with the HYbrid Coordinate Ocean Model (HYCOM) (Metzger et al., 2010), with daily Special Sensor Microwave Imager/Sounder (SSM/I/S) ice concentrations assimilated through Navy Coupled Ocean Data Assimilation (NCODA) (Cummings and Smedstad, 2013). Navy Operational Global Atmospheric Prediction System (NOGAPS) (Hogan et al., 1991) forcing was applied daily to ACNFS prior to 13 March 2013, after which forcing was replaced by the NAVy Global Environmental Model (NAVEM) (Metzger et al., 2013). The ACNFS provides daily 7-day ice products forecasts at approximately a 3.5 km resolution.

CICE uses an elastic viscous plastic (EVP) ice rheology (Hunke and Lipscomb, 2004) to describe the ice dynamics and compute strain rates. It incorporates the standard ridging scheme of Thorndike et al. (1975) to compute the rates of opening, closing, and ridging given the strain rates (Lipscomb et al., 2007). ACNFS calculates the divergence (positive values are divergence, negative values convergence) and shear strain rates as well as the computed opening rate. The strains and opening rates are in units of %/day. Opening rate values vary greatly between 0 (no opening) to more than 1000%/day. Mean values however are on the order of 3%/day, with most

values below. Figure 2 shows the maximum and mean of the daily ACNFS opening rates for the time period of 2010 through 2013. Figure 3 shows the distribution of the opening rate values for the same period.

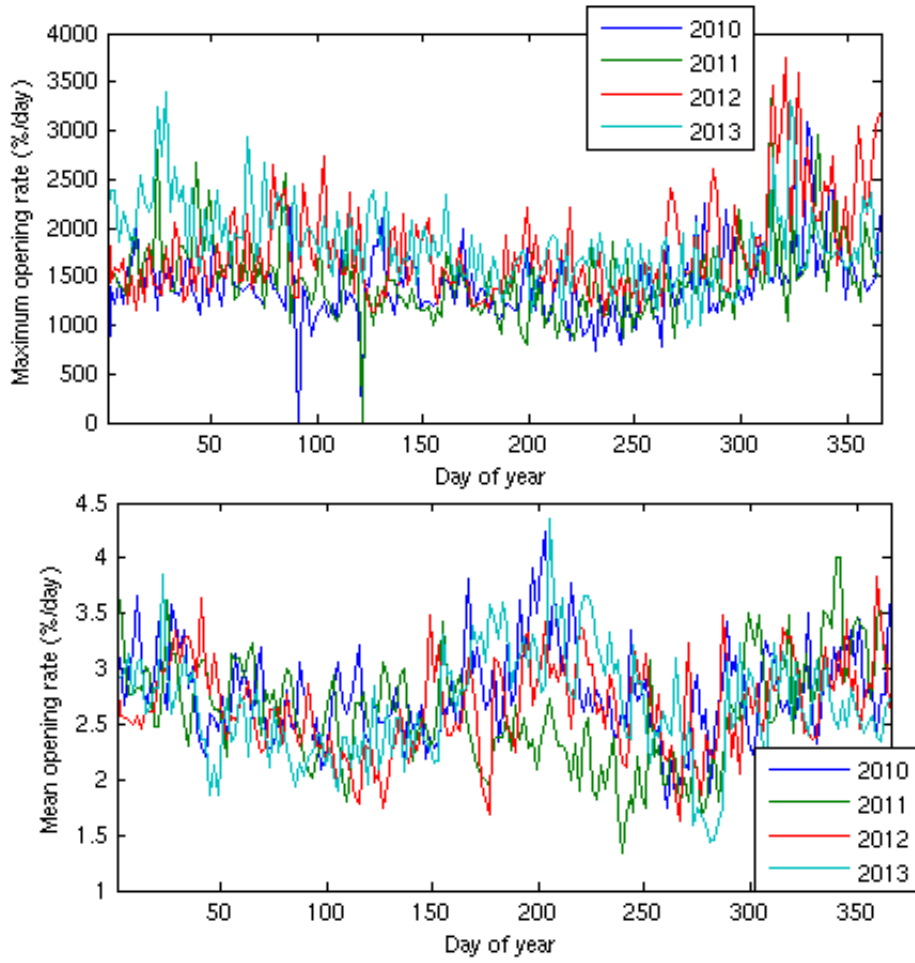


Figure 2: Daily maximum (top) and mean (bottom) opening rate values.

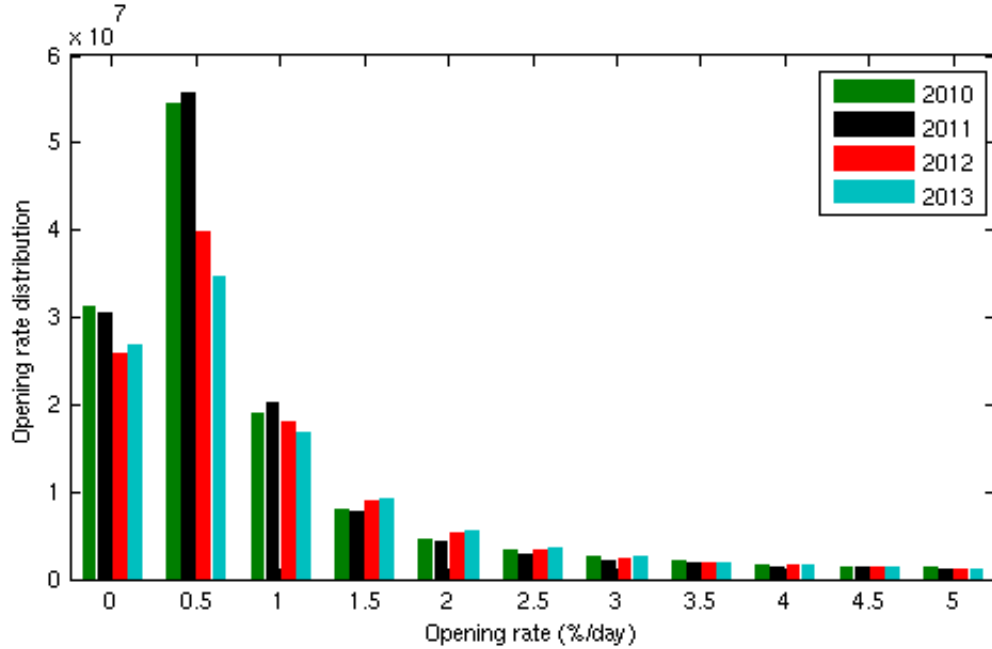


Figure 3: Distribution of opening rate values. Cells with 0 opening rate are not included. The distribution of cells at bin 0 are greater than 0.0 (but less than 0.25).

Figure 4 (a-c) shows the opening rate for a winter day plotted with several color scales. Figure 4a shows the default color scaling of 0 to ~1000%/day. By using this larger color scale, the openings are not easy to identify showing no openings with only a slight hint of color in the Denmark Strait. Figure 4b shows that by reducing the scale closer to the average values (0-15%/day), yields delineated fracture-like features. Figure 4c shows a scale of 0 to 4%/day that was used for most visualization of the opening rates.

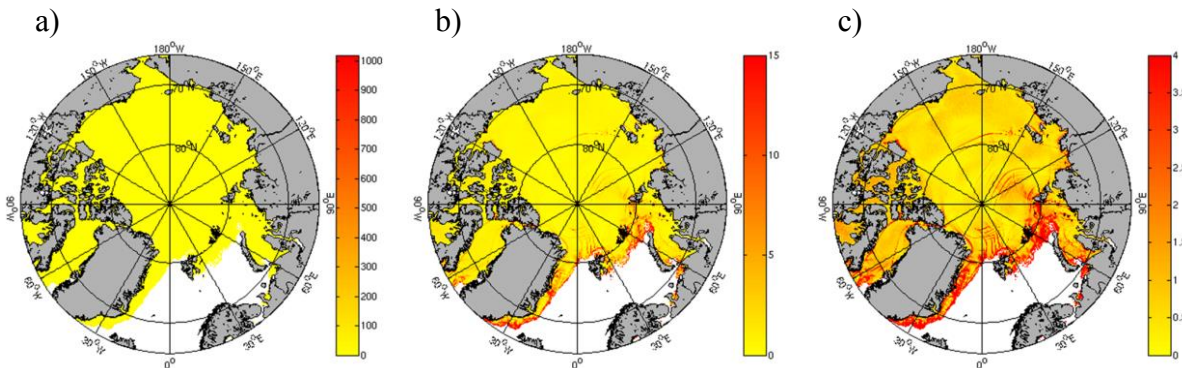


Figure 4: ACNFS opening rate for 00Z January 05, 2012. a) default scale, 0 – max scale. b) scale 0-15%/day. c) scale 0-4%/day.

In preliminary comparisons, the ACNFS opening rate field looked reasonable with features often resembling satellite imagery. Figure 5 shows an example of a typical ACNFS opening rate product illustrating realistic fractures as compared to satellite imagery.

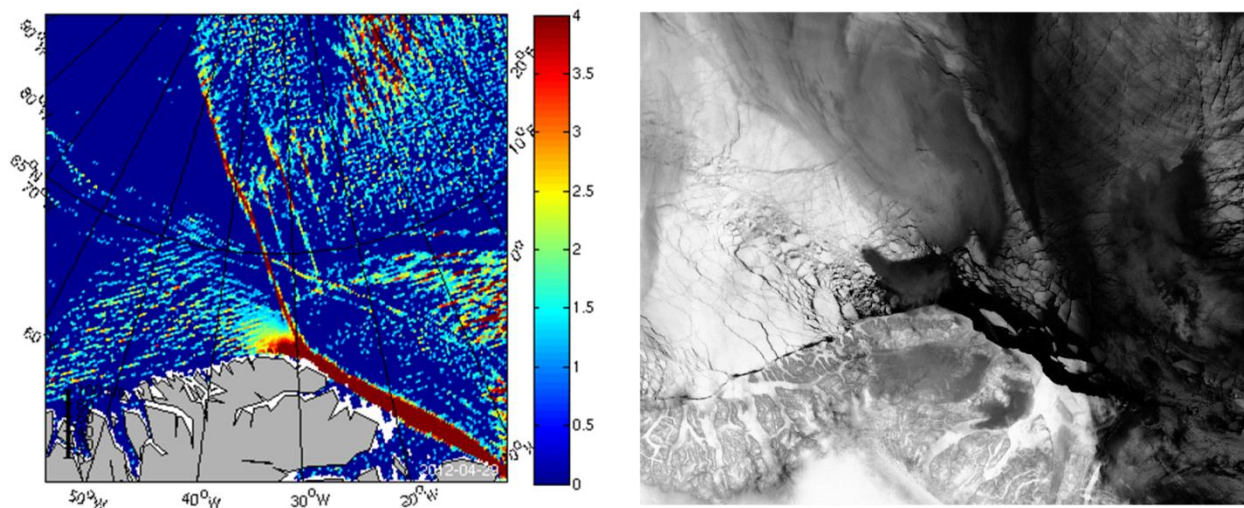


Figure 5: April 20, 2012 ACNFS opening rate (left) and MODIS imagery (right) just off the northern coast of Greenland.

2.2 ACNFS Accumulated Openings

The daily ACNFS model opening rate is an instantaneous value. It provides an indication of how fast an opening event occurs with a unit of percent per day. Unlike imagery, which shows openings that are present, an opening rate is an indication of new or expanding fracturing. The opening rate field does not reflect ice openings from previous days, unless they are expanding or are large enough to be seen in the ice concentration.

For exercise/operations planning and forecasting, knowledge of the timing and location(s) of significant fracturing expected to occur is important. But for daily surface ship and submarine navigation and surfacing, knowledge of where openings are present, or expected is important. To simulate the existing openings and the leads that are opening, an accumulation of opening over the course of a few days is computed. The model does not determine a closing rate, but it does produce a convergence, which is closely related. A more comparable model product can be produced by using the previous 3 days from the time of interest, with opening rates being weighted and then applying any convergence afterwards.

The openings for a day of interest, d is computed for each grid cell separately as

$$O_d = \max\{\omega_d \varepsilon_{A_{d-1}} - \varepsilon_{D_d}, \varepsilon_{O_d}\}, \quad (1)$$

where ε_A is the accumulated opening from the previous day and given by the recursive formula

$$\varepsilon_{A_i} = \max\{\omega_i \varepsilon_{A_{i-1}} - \varepsilon_{D_i}, \varepsilon_{O_i}\}, \quad (2)$$

where i is the day past from the day of interest, ε_O is the opening rate, ε_D is the convergence strain rate, and ω_i is the damping weight applied to the daily opening rate. Expanding Equation 1 for a three day accumulation yields

$$O_d = \max \left\{ \max \left\{ \max \left\{ \omega_{d-3} \varepsilon_{A_{d-3}} - \varepsilon_{D_{d-2}}, \omega_{d-2} \varepsilon_{A_{d-2}} \right\} - \varepsilon_{D_{d-1}}, \omega_{d-1} \varepsilon_{A_{d-1}} \right\} - \varepsilon_{D_d}, \varepsilon_{A_d} \right\}, \quad (3)$$

Figure 6 illustrates Equation 3 for a three day accumulation of openings on a basin-wide scale. Figure 7 illustrates a two day accumulation of openings on a regional scale accompanied with VIIRS imagery for the valid day. Weights of $\omega_i = \{0.8, 0.6, 0.4, 0.2, 0\}$ were chosen for $i = d$ to $d-4$ to reduce the influence of previous openings.

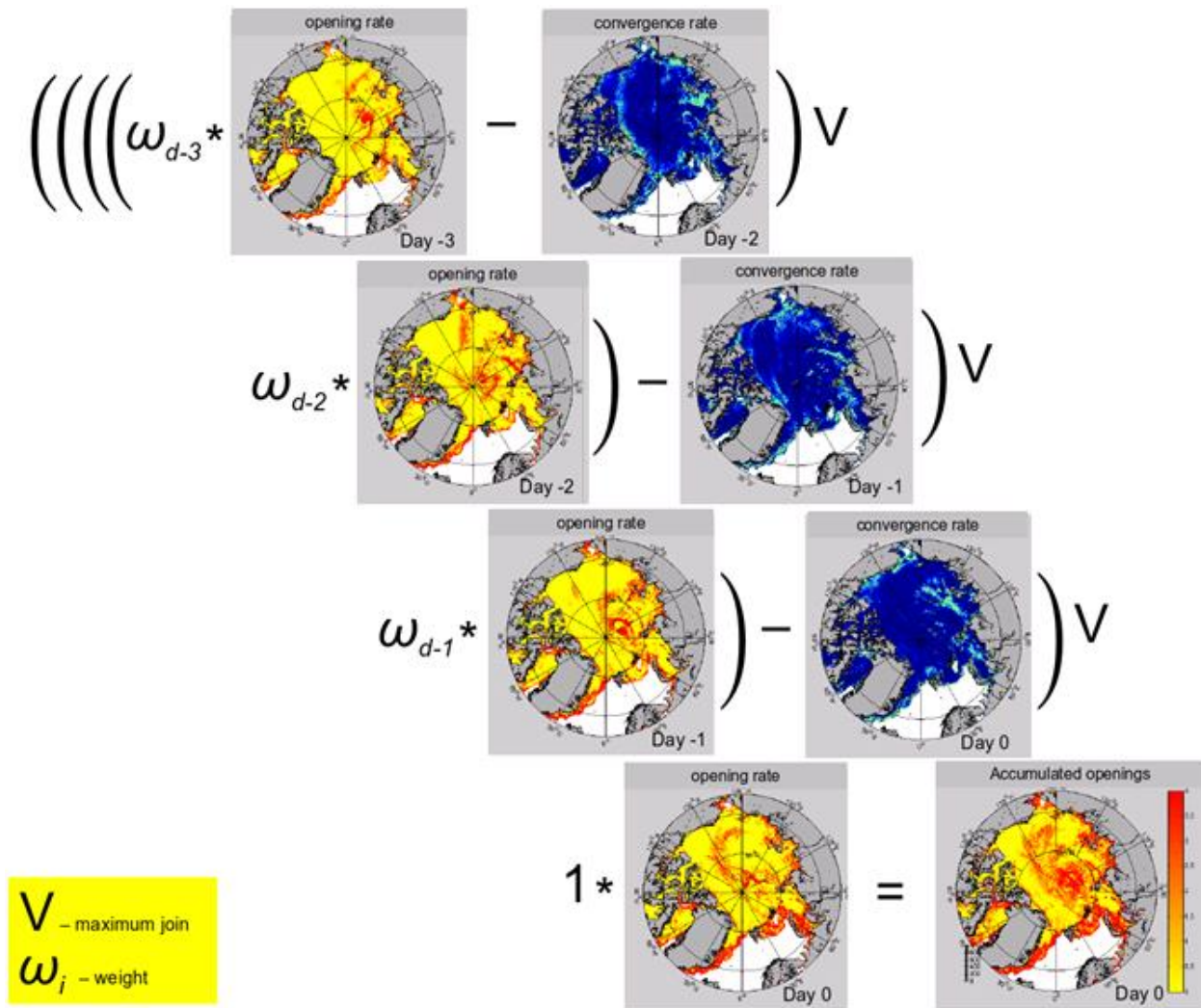


Figure 6: Equation 3 represented pictorially with basin wide openings for May 19, 2014 accumulating 3 previous days of weighted opening rates reduced by convergence rates.

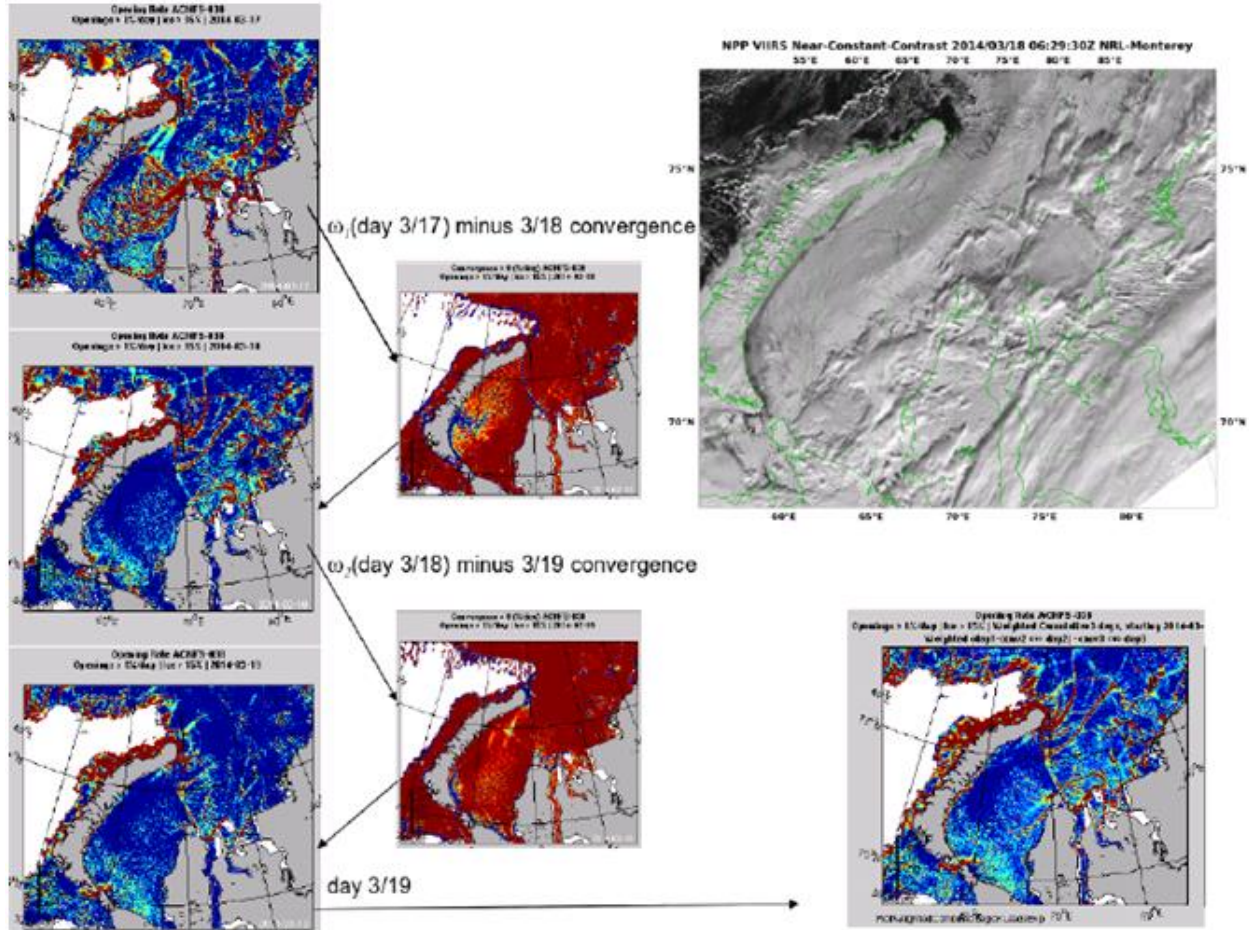


Figure 7: Regional openings for March 19, 2014 accumulating 2 previous days of weighted opening rates reduced by convergence rates. Top right panel shows NPP VIIRS contrast satellite image valid March 18, 2014 (courtesy of NRL – Monterey).

2.3 ACNFS Opening Rate Contours

To assist in the visualization of the fracture field and to provide methods of quantifying the results, the opening rate can be smoothed and contoured. With the ACNFS providing an indication of the general area of openings, rather than individual openings, bounding areas of fractures may yield more reliable results. To capture the area of fracturing on the scales of the FLAP message areas, the contour from an 18 point smoothing filter was used. This contour provided the most consistent fracture grouping. Figure 8 illustrates this contouring with an example of fractures in the Chukchi Sea. The two model plots on the right have the same opening rates plotted with contour overlaid on the lower plot.

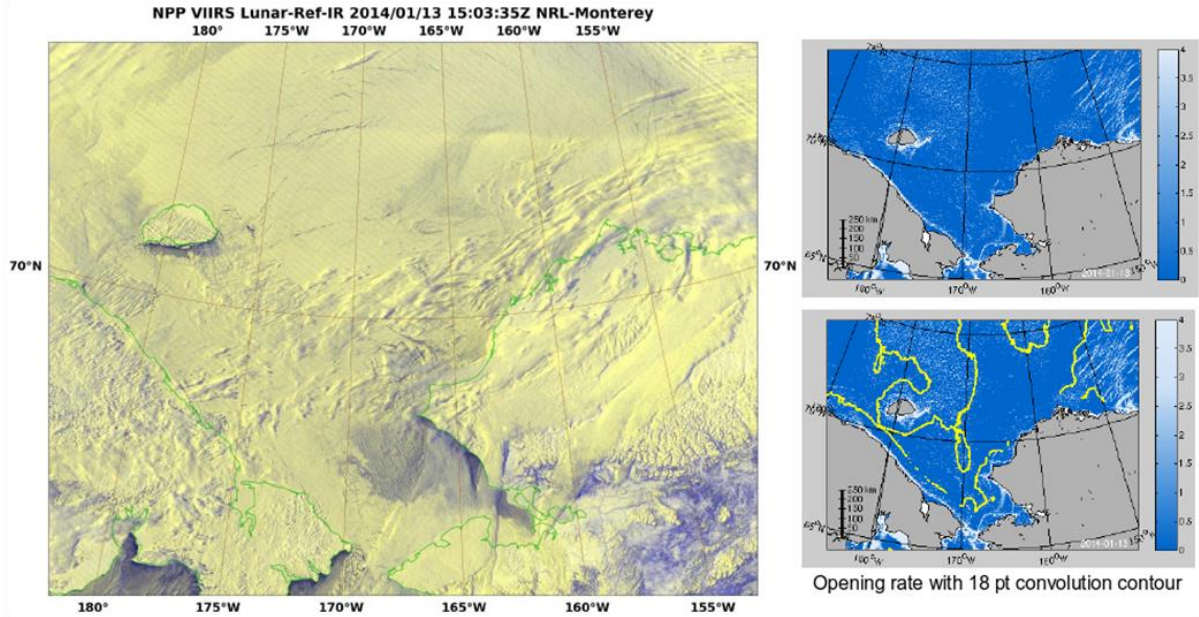


Figure 8: Clockwise from left: VIIRS imagery of Chukchi Sea January 13, 2014 (Courtesy of NRL/Monterey); ACNFS opening rate for same date; ACNFS opening rate for same date with opening rate contour overlaid.

3 Validation

The ACNFS operational sea ice model is evaluated primarily on the basis of its ability to capture Naval Ice Center (NIC) identified Fracture/Leads, and Polynyas (FLAP). The NIC FLAP dataset consists of 81 FLAP messages from January 2012 through November 2012. The FLAP text messages delineate areas of openings in the ice on a tactical scale, hand-drawn by NIC ice analysts from available satellite imagery including Envisat and RADARSAT-2 (SAR); and MODIS and DMSP/OLS (visible). The messages can cover a sub-region of the Arctic or can be basin wide. The messages contain coordinates of poly-line segments identifying fracture area polygons and polynya area polygons. If predominant, orientations of fractures and/or ice types are noted. In total, 227 fracture polygons and 37 polynya polygons are identified. Coordinates north of 82° were given in transpolar coordinates (where the north pole (90/0) is centered instead at Greenwich mean time and the equator) and converted to standard Greenwich coordinates.

As described in Section 2.1, ACNFS consists of 3 components: 1) ice – CICE, 2) ocean – HYCOM and 3) data assimilation – NCODA. The model provides a daily 7-day forecast at approximately 3.5 km resolution. For the FLAP comparisons, the model output from the 2-day hindcast (best quality) is used. ACNFS opening rates are used as the primary source of comparison and are indicative of the amount of fracturing and lead distributions.

The CICE model has also been implemented into the Global Ocean Forecast System (GOFS 3.1) (Metzger et al, 2014). GOFS 3.1 is comprised of the 1/12° global HYCOM and the NCODA system of which ACNFS domain is a subset and is likewise forced with NAVGEM atmospheric forcing out to 7 days. GOFS 3.1 provides nowcasts and forecasts of the global ocean environment which includes three-dimensional ocean temperature, salinity and current structure, surface mixed layer, the location of mesoscale features, ice concentration, thickness and ice drift.

GOFS 3.1 has the capability to provide ice forecasts in the Southern Hemisphere as well as the Northern Hemisphere. GOFS 3.1 opening rate products are also validated as part of this validation test report. GOFS 3.1 passed validation in September 2014, with transition to NAVOCEANO scheduled by 2014 year's end.

3.1 Thresholds

Several thresholds were determined to best capture the fracture fields: 1) the scale in which to view the plots, 2) the minimum opening rate to consider an opening, and 3) the concentration in which to consider openings. As shown in Figure 2, the maximum opening rate over the Arctic basin on any given day is between 1000 and 3000 %/day, with extremely high opening rate values isolated generally near the ice edges. Figure 9, similar to Figure 4, shows the opening rate output for another typical Arctic day plotted at different scales. Plotted to the maximum for this day of 1510 %/day (Figure 9, left), no fracturing is evident. When scaled to a much lower value of 50 %/day (Figure 9, middle), only a few openings are seen along the ice edge. Ultimately at a scale from 0 to 4 %/day (Figure 9, right), the openings are easily viewable. Reasonable scales limits were shown to be between from 0 to 3 – 15 %/day. The NIC and NRL agreed to use a scale from 0 to 4 %/day for the opening rate validation.

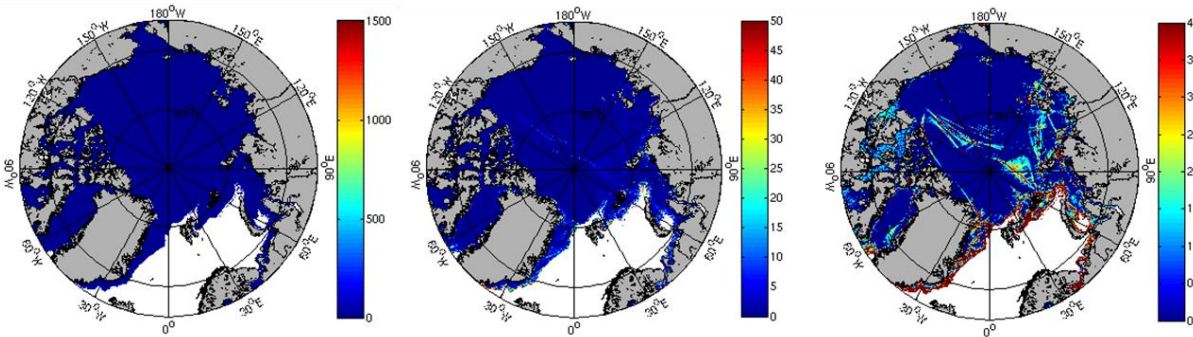


Figure 9: ACNFS opening rate plotted at different scales. Left: 0 to the maximum opening rate of 1510 %/day. Middle: 0 to 50 %/day. Top: 0 to 4 %/day.

Opening rate values have a minimum of 0 %/day indicating no opening, but almost all grid cells have an opening rate component, even if extremely small. Choosing a minimum as any opening greater than 0 (or a small value) is not representative of the fracturing, as it implies fracturing throughout. A minimum opening rate of 1 %/day was chosen as best mirroring fracture regions at the scale seen in imagery and in a typical FLAP messages. Figure 10 illustrates the consequences of the minimum opening rate. Cells are colored green for opening rates greater than the threshold and cells are colored red for opening rates less than the threshold. The left plot has a minimum threshold of 0.1 %/day. Only a few isolated cells have values less than the minimum. The middle plot has a minimum threshold of 0.5 %/day. Some opening structure is becoming visible, but it is still not a reasonable indication of actual ice openings. The right graphic shows a minimum threshold of 1 %/day.

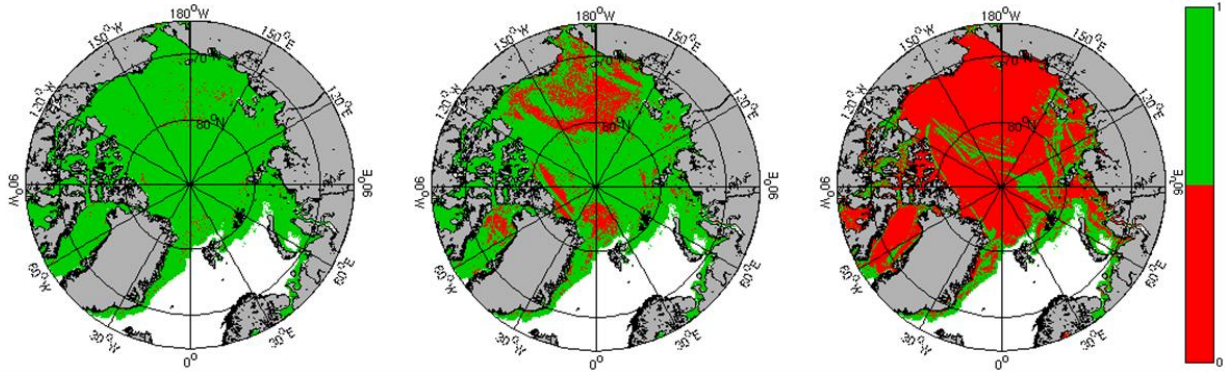


Figure 10: ACNFS openings greater than different threshold values. Left: opening rate > 0.1 %/day. Middle: opening rate > 0.5 %/day. Top: opening rate > 1.0 %/day.

3.2 Model Best Quality

The operational ACNFS (run at 18Z) produces a daily nowcast and 7 day forecast at time 00Z from the previous day's 24 hr restart file. Every day the system reaches back 72 hours from the nowcast time (18Z) to use any late arriving satellite data. As a result, ACNFS produces three hindcasts: time 00Z on the model run day, a 1-day hindcast, and a 2-day hindcast. The 2-day best quality hindcast is considered the model's best representation of the actual ice conditions and is used in the comparison against the FLAP messages

3.2.1 FLAP Message Validation

Ice openings were examined through an initial qualitative analysis comparing distributions of areas of ACNFS opening rates and FLAP messages. For each message, the number of fractures and polynyas along with the density and orientation noted and the satellite imagery used in the analysis were listed. Comparison metrics were compiled for each message fracture area noting the model agreement category as strong match, partially covered, location off, subset of field, or no match. Table 1 (shown below) presents the summary statistics comparison categories totals. The first three columns are the gross number of fracture regions identified in the FLAP messages that went into the statistics. The rest of the columns are percentages of the fracture regions. Matches are classified as strong (“√”), meaning the model contained fracturing in the same location as the FLAP message polygon; to some degree (“?”), broken down further into off-set location, partial area match, subset of area matched, and weak openings in area; and poor match (“×”). The “√/?” column is the sum of the strong and to some degree columns. The metrics suggest that the ACNFS accumulated openings were an improvement over the instantaneous opening rate and that ACNFS and GOFS 3.1 performed similarly. In all cases, the models did well, capturing between 88-97% of the FLAP fracture regions, with ~ 30% as a strong match. Using the accumulated openings improved the miss-rate considerably.

	Fracture Regions			Percent of Fracture Regions							
	✓	?	X	✓	?				?	✓ + ?	X
					off-set	partial	subset	weak			
ACNFS opening rate	49	89	18	31%	5%	21%	22%	9%	57%	88%	12%
GOFS opening rate *	42	85	33	26%	4%	21%	18%	10%	53%	79%	21%
ACNFS accumulated openings	67	95	6	40%	3%	10%	40%	4%	57%	97%	4%

Table 1: FLAP area prediction comparison categories totals “✓” indicated a strong match; “?” indicates a match to some degree, and “X” indicates a poor match. “?” is broken down further into off-set location, partial area match, subset of area matched, and weak openings in area. (* GOFS best quality is a 1-day hindcast.)

There are intrinsic limitations in the assessment of the model performance against the FLAP messages. The poly-lines in the messages are subjective, hand drawn borders made by different analysts, under different circumstances, with different and unknown intelligence/tactical needs, and with different and unknown source imagery. If a model opening area is not included in a FLAP message, there is no way to know whether or not it exists. In the absence of consistently clear imagery or other ground truth data, the FLAP messages are the best validation data.

3.2.2 RADARSAT Model Analysis

Some publicly available basin-wide RADARSAT-1 data transformed into estimates of ice motion and deformation by NASA’s RADARSAT Geophysical Processor System (RGPS) (Lindsay and Stern, 2003) coincides with available ACNFS runs. The RGPS and ACNFS products are available during winter.

The RGPS deformation fields were generated over weekly time periods rather than daily. To compare the daily model output with the weekly data, the ACNFS output strain rates (opening rate, divergence, and convergence) were accumulated over the weekly time period to capture all openings (closings). Ice drift u- and v- components along with a calculated magnitude were averaged over the time period. Typical results are shown in Figure 11, with the model indicating openings in the same general areas as the RADARSAT divergence, but without the same structures. The ACNFS and the RADARSAT ice drift motion correlate fairly well on the gross scale.

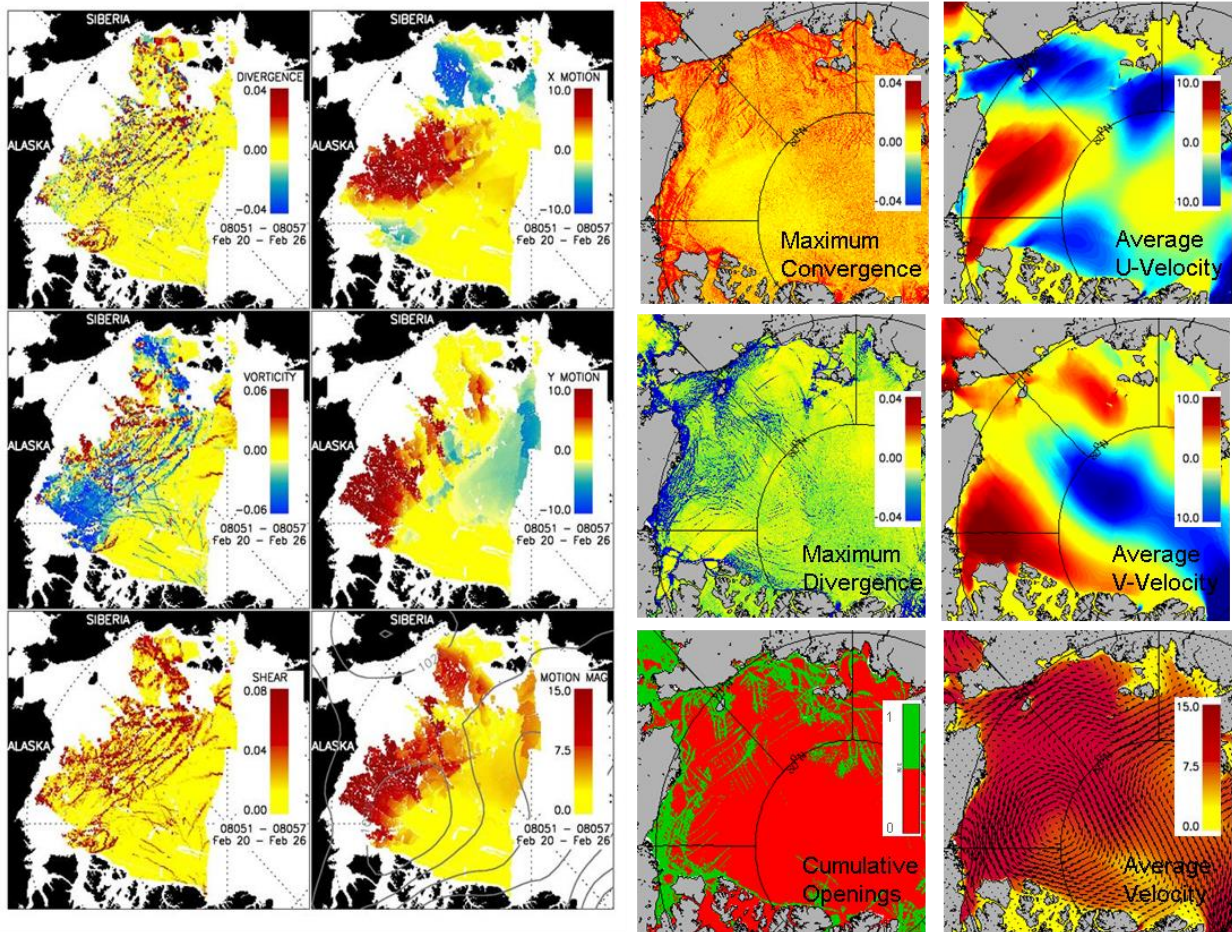


Figure 11: February 20 to February 26, 2008 deformation and velocity fields from RADARSAT processing system (left 6 panels - RADARSAT and the ACNFS model fields (right 6 panels). Panels indicate the following: RADARSAT: top left – divergence (+)/convergence (-), top right – u-component velocity, middle left – vorticity, middle right – v-component velocity, bottom left – shear, bottom right – ice drift magnitude. ACNFS: top left – maximum convergence, top right – average u-component velocity, middle left – maximum divergence, middle right – average v-component velocity, bottom left – cumulative opening and bottom right – average ice drift velocity.

3.3 Forecasting

Section 3.3 indicates how well ACNFS performed in capturing the known ice openings in forecasting the opening rate out for 7 days. The forecast validation covers the period of February 2014 – July 2014. The forecasts were validated on a full Arctic scale against reference 2-day hindcasts and compared with persistence. On a regional scale, the model was compared against events of the Commander, Submarine Forces (COMSUBFOR) ICEX 2014 exercise.

The validation shows that the ACNFS forecasts provide value added over persistence even out to 6 day, performing particularly well in the first 24 to 48 hours, and then degrading out though the 7 days.

3.3.1 Reference Hindcasts

In the absence of ground truth data (no FLAP messages) during the time period that model forecasts were available, the ACNFS 2-day hindcasts were used as the reference data for the model forecasts. The 2-day hindcast is considered the model's best representation of the true ice conditions.

3.3.1.1 Visual Inspection

In determining the forecast skill for ACNFS opening rates, several weeks of forecasts over several months were examined, both on the full Arctic and regional scales.

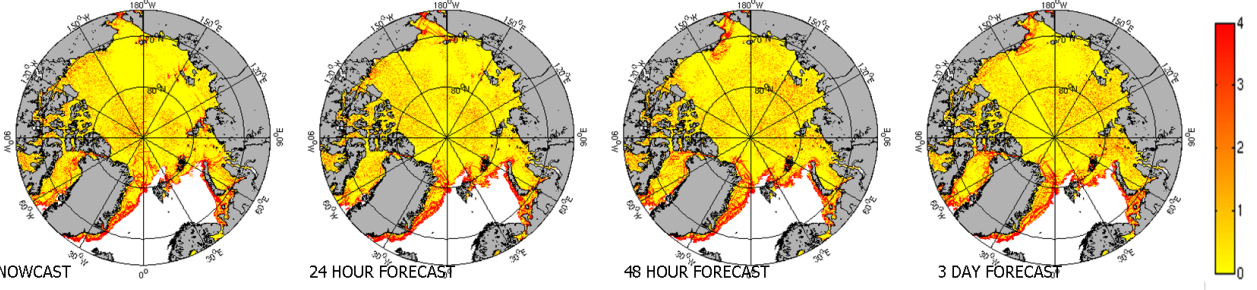
Figure 12 shows a sample 7-day forecast of opening rate for the second week in February 2014. The reference hindcasts are shown directly below the forecasts. The model does extremely well through the first 24 hour forecast and still very well out through 4 days. By the 7th day, the model forecasted opening rate product has degraded. Figure 13 shows the corresponding 7-day forecast of ice drift. The same trend is clearly seen in the ice drifts, with the 7th day drift being drastically different. The 7th forecast day was often inconsistent due to the model 7th day forcing not being available at run-time. In this case, the model reverts to climatological forcing.

Figure 14 is the forecast for a month later in March 2014. In this case, the model does extremely well out through 4 days and very well out though the 6th. As with the previous example, by the 7th day, the model did not do well. The corresponding ice drifts are shown in Figure 15. The ice drifts were well captured out through 5 days.

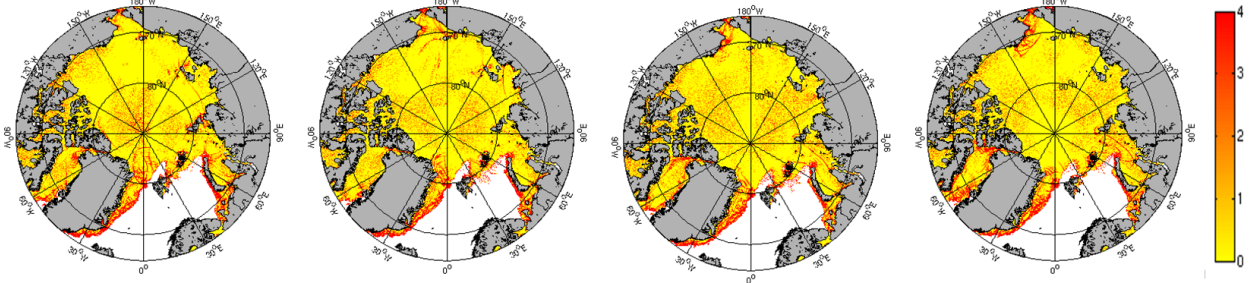
Examining ACNFS on a smaller scale, Figure 16 zooms into the Kara Sea region where more fracture details can be seen and differences are more visible. The model did very well out to 3 days, but for the 4-7 day forecasts, the model forecast did not do as well. By the 7th day the model picked the fracturing back up. A look at the forecasted air stress (Figure 17) reveals why the opening rate got off after 3 days, the air forcing was very different for 4 through 7th forecast days.

The samples shown are typical forecasts and representative of the initial correlation and then gradual degradation of the forecast.

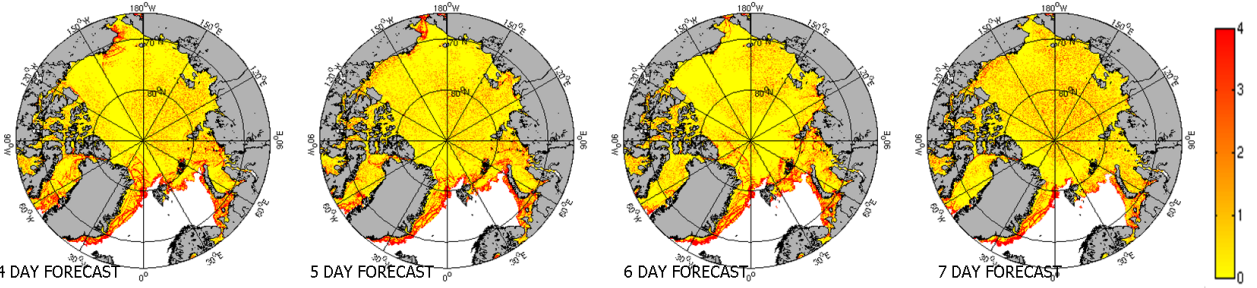
FORECASTS



REFERENCE HINDCASTS



FORECASTS



REFERENCE HINDCASTS

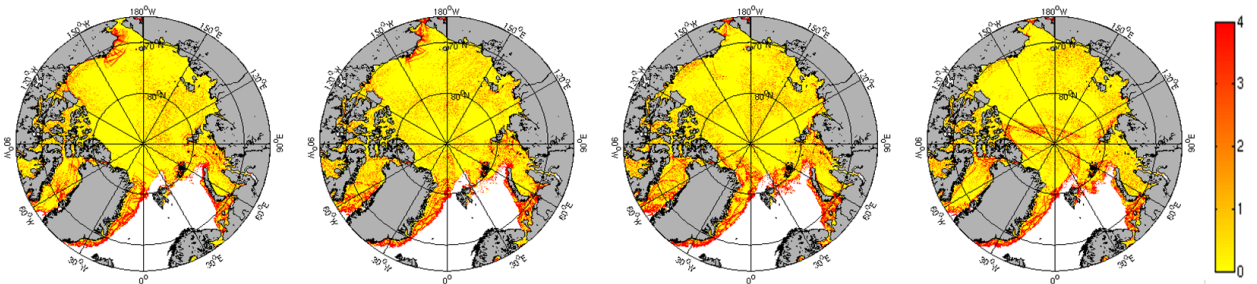
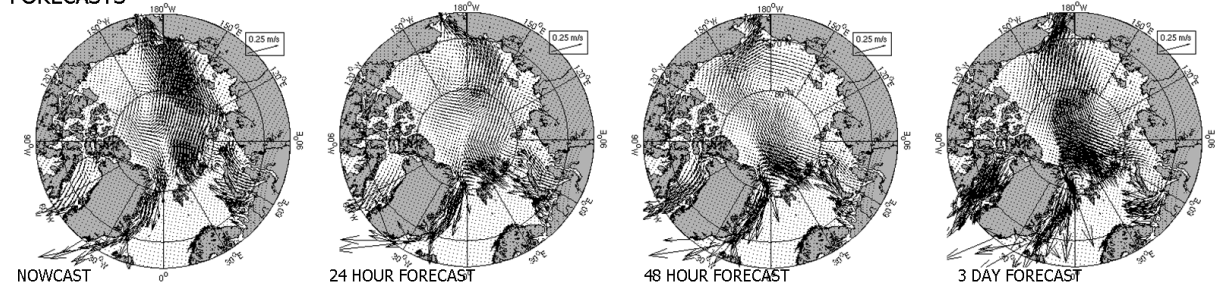
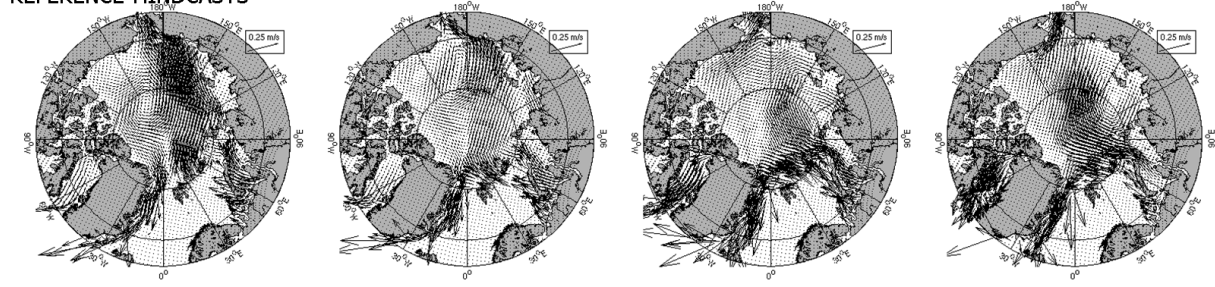


Figure 12: Forecast and Reference opening rate plots from February 13, 2014 nowcast.

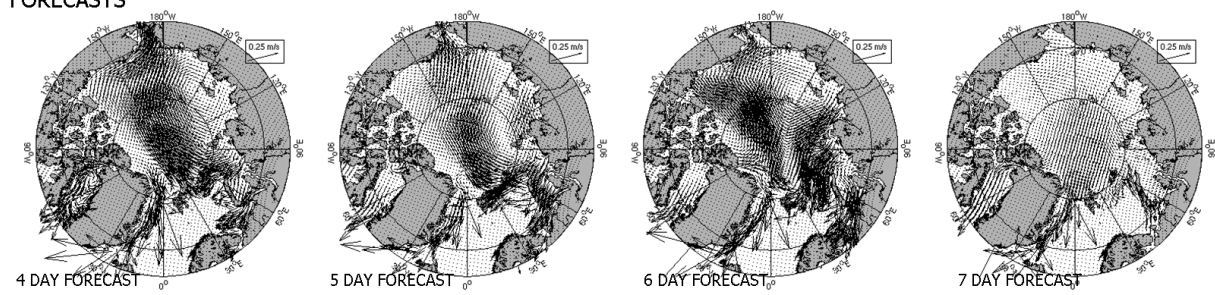
FORECASTS



REFERENCE HINDCASTS



FORECASTS



REFERENCE HINDCASTS

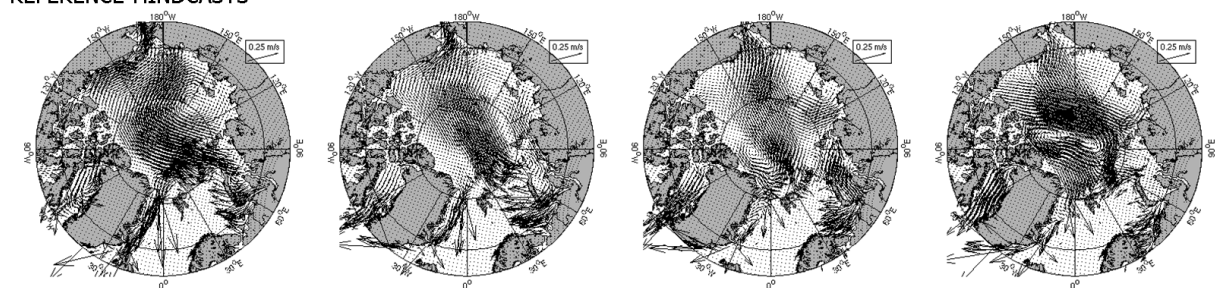
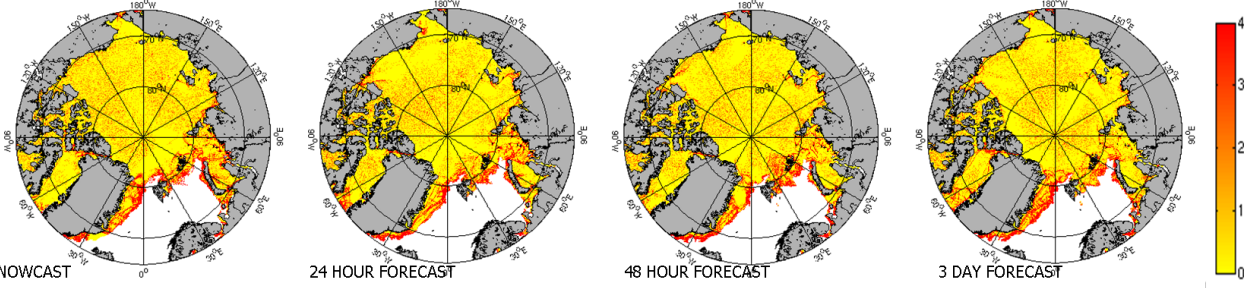
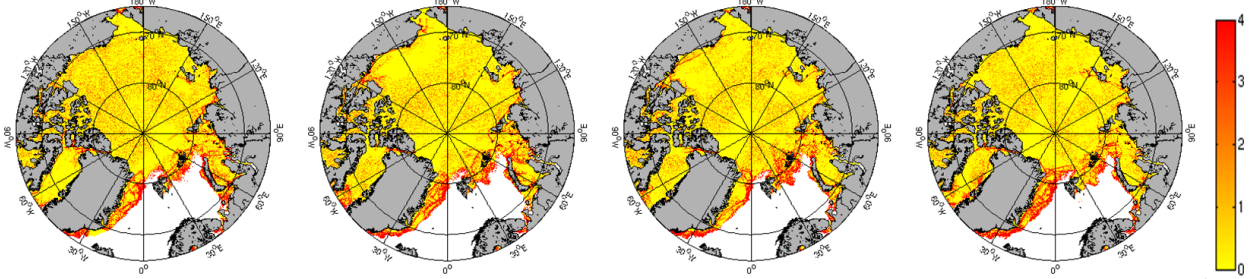


Figure 13: Forecast and Reference ice drift plots from February 13, 2014 nowcast.

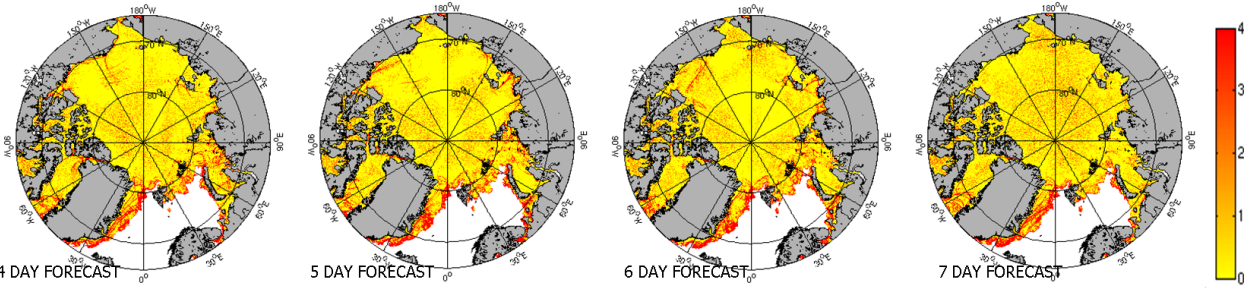
FORECASTS



REFERENCE HINDCASTS



FORECASTS



REFERENCE HINDCASTS

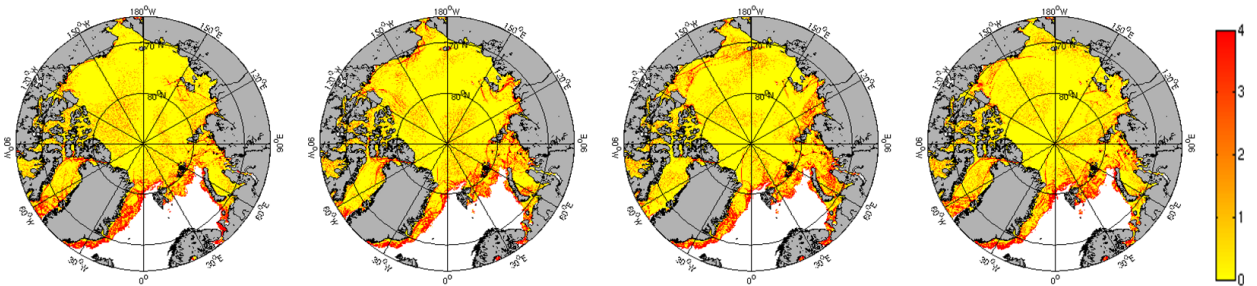
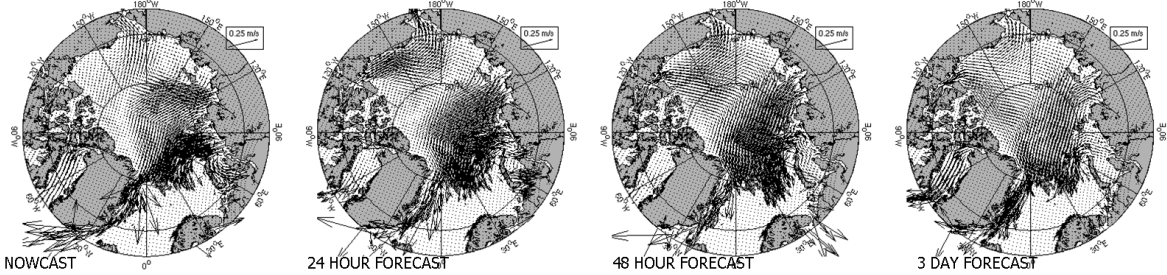
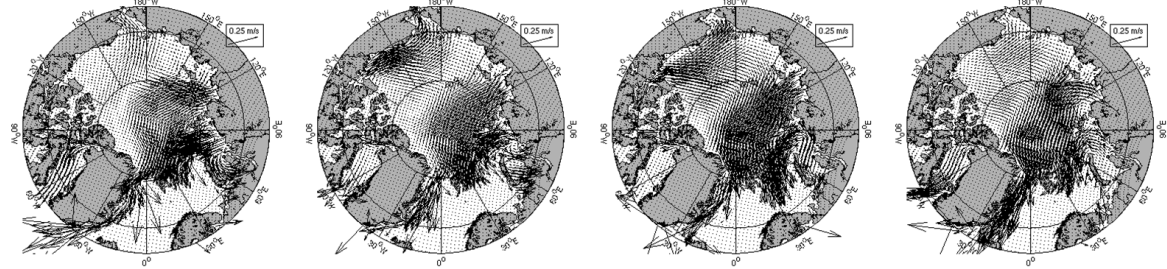


Figure 14: Forecast and Reference opening rate plots from March 11, 2014 nowcast.

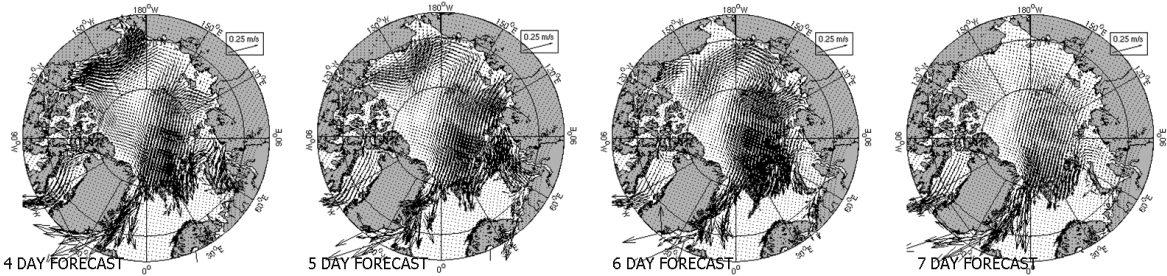
FORECASTS



REFERENCE HINDCASTS



FORECASTS



REFERENCE HINDCASTS

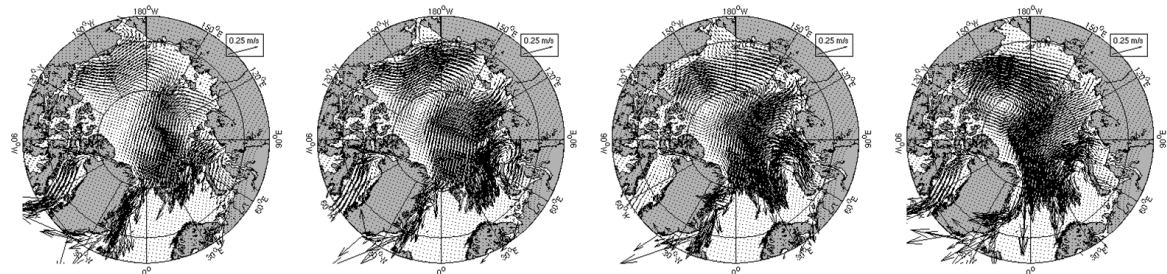
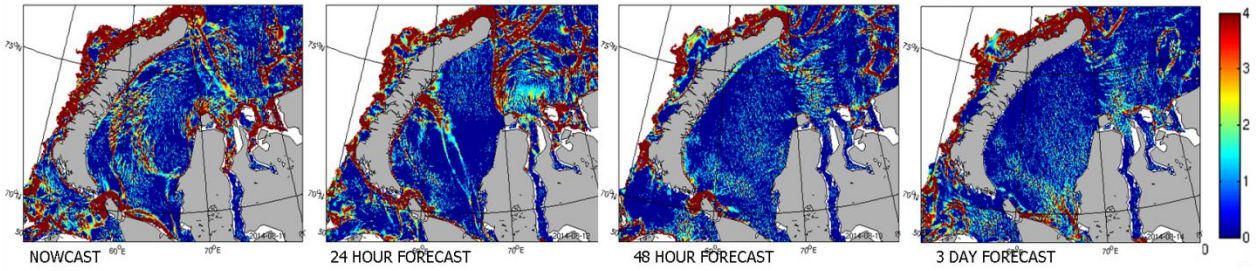
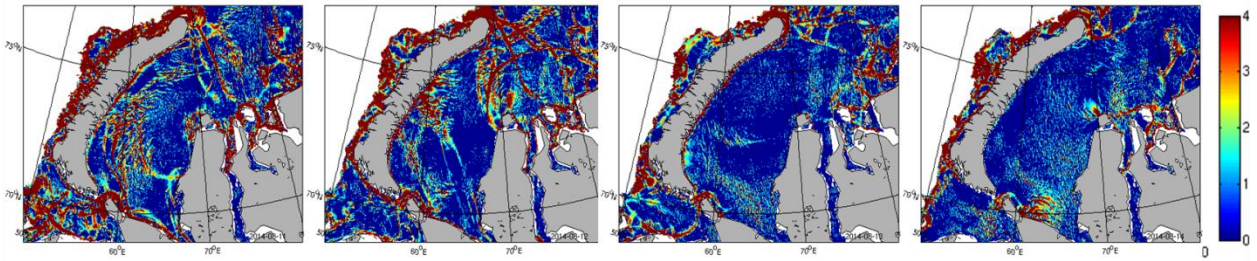


Figure 15: Forecast and Reference ice drift plots from March 11, 2014 nowcast.

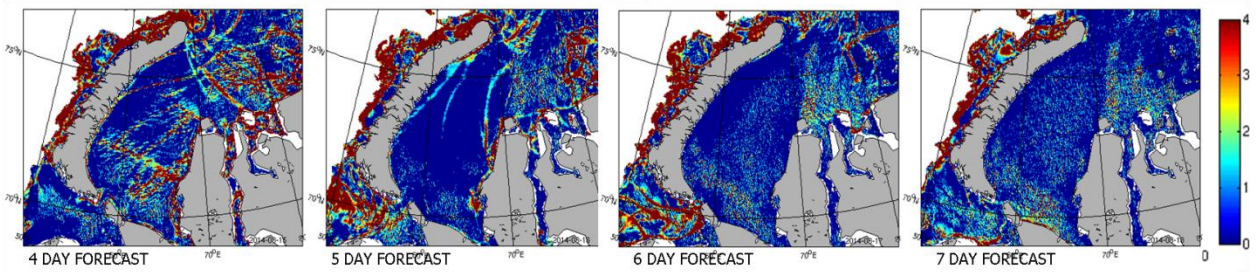
FORECASTS



REFERENCE HINDCASTS



FORECASTS



REFERENCE HINDCASTS

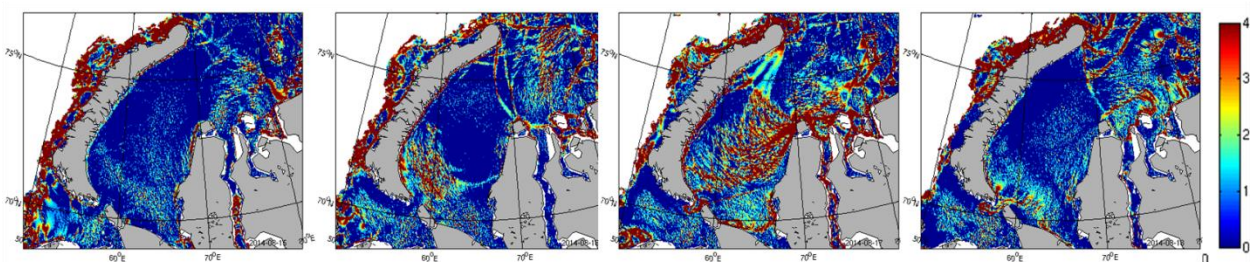
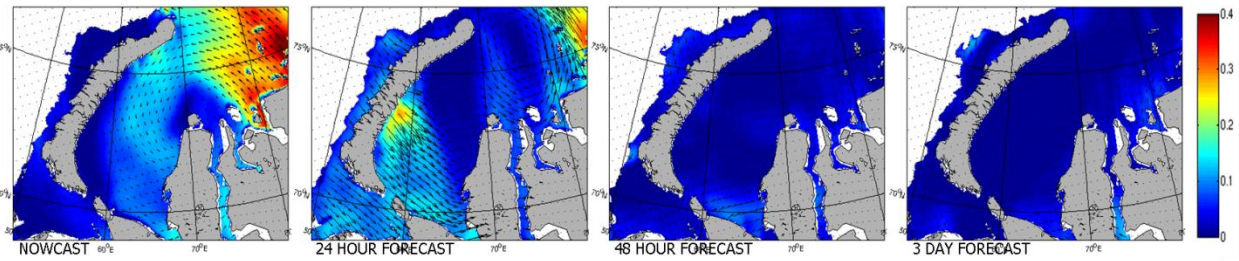
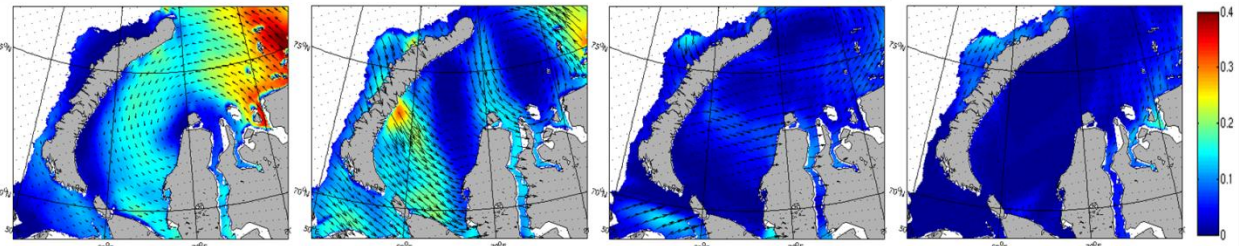


Figure 16: Forecast and Reference opening rate plots from March 11, 2014 nowcast for Kara Sea.

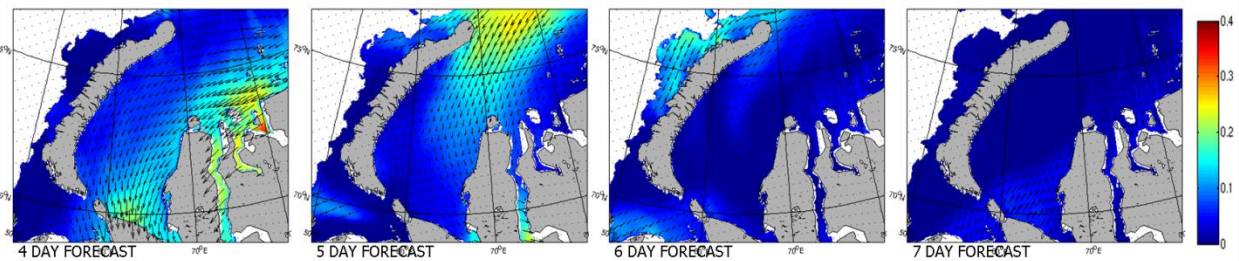
FORECASTS



REFERENCE HINDCASTS



FORECASTS



REFERENCE HINDCASTS

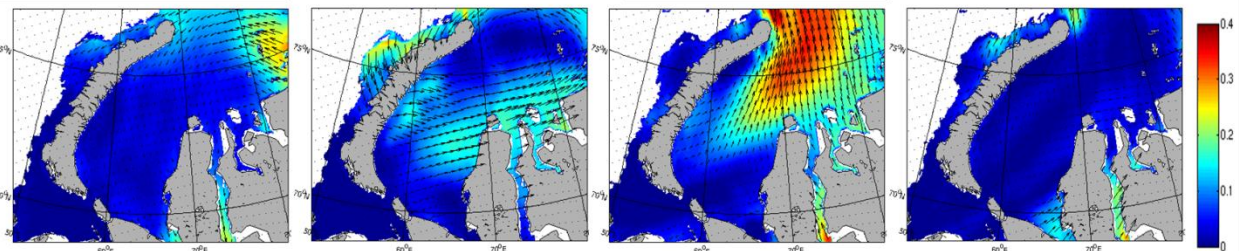


Figure 17: Forecast and Reference air stress plots from March 11, 2014 nowcast for Kara Sea.

3.3.1.2 RMSE

Validation is also performed by analyzing statistically the agreement between the forecasts and the reference hindcasts. The Root Mean Square Error (RMSE) was computed for the sample forecasts and is shown in Figure 18. The hindcasts are included in the computations and are shown as negative forecast days. The reference hindcast is shown as -3 days with an error = 0. The daily nowcast analyses are shown at day 0 with the forecast days to the right. The forecast clearly performs better within a shorter forecast period and degrades with time. The RMSE growth rate is consistent between forecasts, with only a few exceptions and is highest between the nowcast and the 1-day forecast. After the 1-day, the forecasts have a decreasing slope,

becoming flat by the 7th day.

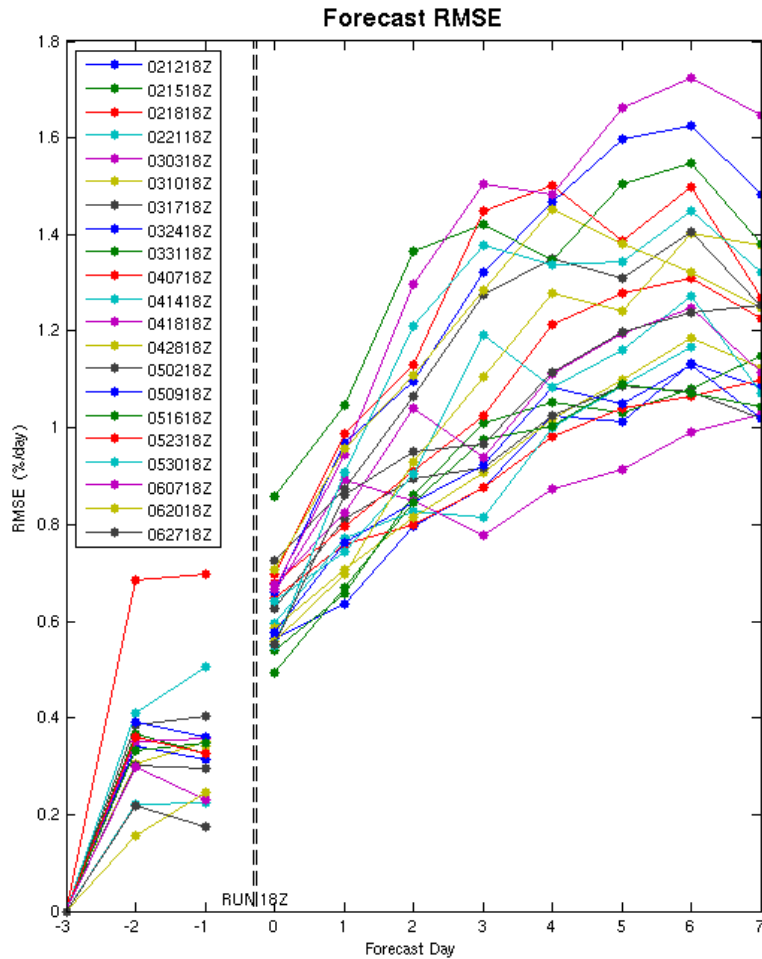


Figure 18: Root Mean Square Error of the opening rate forecasts. Forecast time periods are from February through June 2014.

3.3.1.3 Contingency Validation

Since observed fracturing consists of the presence or absence of a fracture in an area, the accuracy is assessed by comparing the forecasts with a binary classification of opening and non-opening areas of the reference analysis for the forecast time. The comparison of reference and forecast model results classified into 2 classes is represented through contingency tables. Table 2 shows the contingency table used to score the forecast performance against the reference hindcast.

		Reference Standard	
		Opening	Not opening
Forecast	Opening	true positive	false positive
	Not opening	false negative	true negative

Table 2: Contingency table used for forecasting ice openings.

To reduce the opening rate values to an opening/non-openings classification, a cut-off value is needed. As discussed in Section 3.2.1, the model is used to provide an *area* of openings rather than openings for individual grid cells. To closely match the scale of the fracture areas in the FLAP messages, the same smoothing that was applied to capture the fracture fields is used in the contingency metrics. After experimenting with filters and cut-off values, a cut-off opening rate value of 0.5 %/day applied after the 18 point smoothing filter was selected to best represent the FLAP contours. Figure 19 illustrates the effect of the cutoff value. The 0.25 %/day threshold yields a basin almost entirely covered by fracture areas. On the other end, a 1.0 %/day threshold yields a basin almost entirely void of fracture areas. A 0.5 %/day threshold yielded the most reasonable fracture areas.

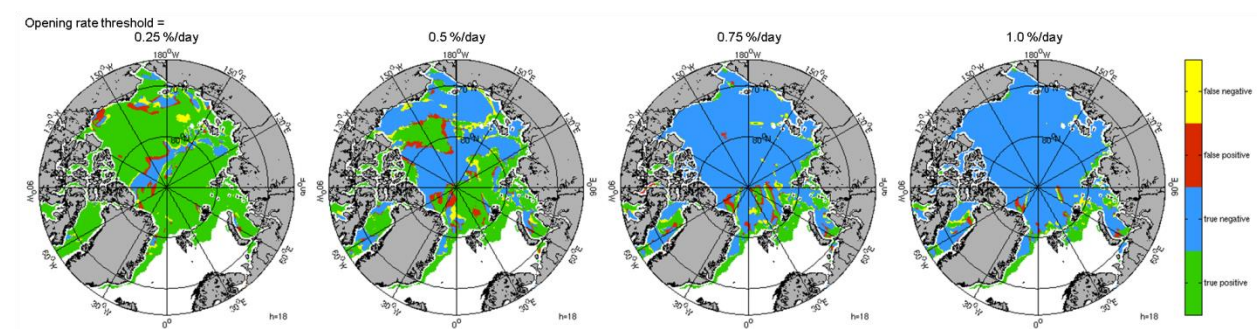


Figure 19: Contingency plot threshold selection.

By combining correctly and incorrectly classified openings and non-openings, quality measures can be derived. To analyze ACNFS FLAP-like product capability, contingency plots were made and statistical quality metrics of their overall accuracy, sensitivity, and specificity accumulated.

$$\text{Accuracy} = (\text{True Positive} + \text{True Negative}) / \text{All Positive and Negative.}$$

$$\text{Sensitivity} = \text{True Positive} / (\text{True Positive} + \text{False Negative}).$$

$$\text{Specificity} = \text{True Negative} / (\text{True Negative} + \text{False Positive}).$$

Preliminary results (February through June 2014) are very promising and show that the model does very well in the first 1 - 4 forecast days with generally over 80% sensitivity and then tapers off slowly from there as opposed to persistence which only has about 50% sensitivity for the 24 hours forecast. Figure 20 plots the forecast contingency accuracy metrics out to 7 forecast days. Individual forecasts are shown in grey and the mean of the forecasts in black.

Sensitivity is a measure of how well a test was at detecting a condition. A high sensitivity in this context implies that the model did well predicting opening cells. The sensitivity is very high for the nowcast and drops off quickly, fairly linearly with each day further out. The often inconsistent 7th forecast day is due to the model 7th day forcing not being available at run-time. In this case, the model reverts to climatological forcing.

Specificity is a measure of how well a test correctly identifies the absence of a condition. A high specificity implies that the model did well predicting non-opening cells. The specificity is very high for the nowcast and 24 hour forecast and drops quickly for the next 48 hours. After that a slower drop-off in specificity is seen.

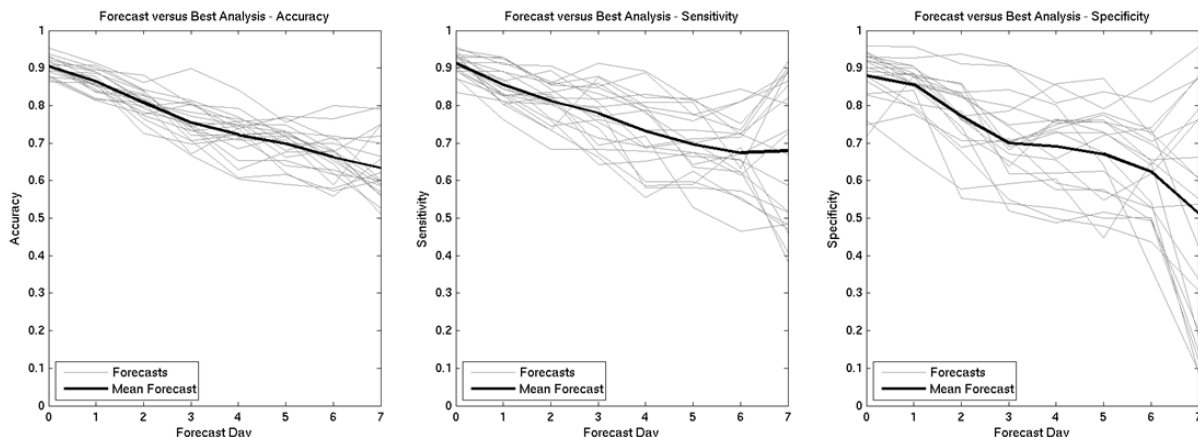


Figure 20: Daily and mean accuracy, sensitivity, and specificity of ACNFS model forecasts out to 7 days. (February through June 2014)

3.3.2 Persistence versus Model Forecast

To provide context to the performance of the model forecast predictions, the ACNFS opening rate forecasts were compared against persistence. Persistence assumes no skill in forecasting. The last known condition, in this case the reference hindcast opening rates for the day prior to the nowcast day, is held constant for all forecast days. The same statistics used to analyze the model forecasts were calculated for the persistence forecasts. As expected, the RMSE, accuracy, sensitivity, and specificity statistics show that the ACNFS forecasts performed better than persistence. This improvement extended out to 6 forecast days. By the 7 day forecast, persistence had almost caught up to the model forecasts. Figure 21 and Figure 22 shows the improvements in model forecasting relative to persistence. Individual forecasts and their corresponding persistence are shown in matching colors. Mean persistence and model forecasts

are shown in black.

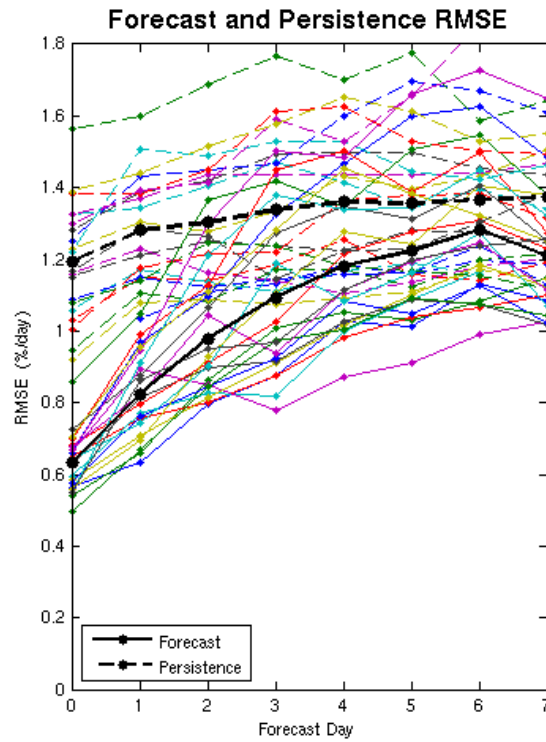


Figure 21: Persistence and model forecasts RMS Error in opening rate. (February through June 2014)

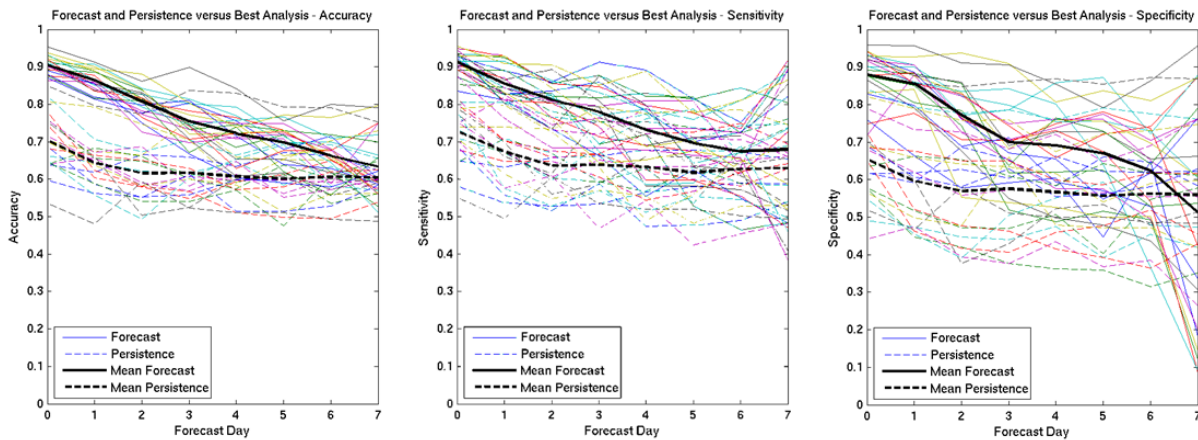


Figure 22: Daily and mean accuracy, sensitivity, and specificity of ACNFS model forecasts and ACNFS persistence out to 7 days. (February through June 2014)

3.3.3 U.S. Navy Arctic Submarine Laboratory Ice Exercise (ICEX)

Navy submarines have conducted under-ice operations in the Arctic regions in support of inter-fleet transit, training cooperative allied engagements and operations for more than 50 years. Since 1958, the U.S. Submarine Force has completed more than 120 Arctic exercises. U.S. Navy

Arctic Submarine Laboratory Ice Exercise (ICEX-2014) began on March 17, 2014 and was built into an ice floe north of Prudhoe Bay, Alaska and was scheduled to continue through March 30, 2014. However, large shifts in the prevailing wind direction between March 18th and March 20th created instabilities in the wind-driven ice floes on the Arctic Ocean which led to multiple fractures in the ice near the camp. These cracks prevented the use of several airfields used for transporting personnel and equipment to the ice camp. The rapidly changing conditions of the ice, along with extremely low temperatures and poor visibility hampered helicopter operations and made sustaining the runway potentially risky. Because of this the Commander, Submarine Forces (COMSUBFOR) announced an early end to the ICEX-2014 on March 23.

Examining the ACNFS/NAVGEN forecasts leading up to the events show that large-scale fracturing was predicted 24 to 48 hours prior to events and the strong winds and wind reversals predicted up to 6 days in advance. Ice fractures were already prevalent in the general area in the weeks leading up to the exercise, but strong shifts in winds brought more. Strong easterly winds picked up across the Beaufort March 15th and 16th and a strong reversal of winds occurred March 20 to 21st, forcing the shut down of operations.

Figure 23 shows the increase in strong easterly winds on March 15th and 16th reflected in the ACNFS air stress. The general area of the ice camp is outlined in red.

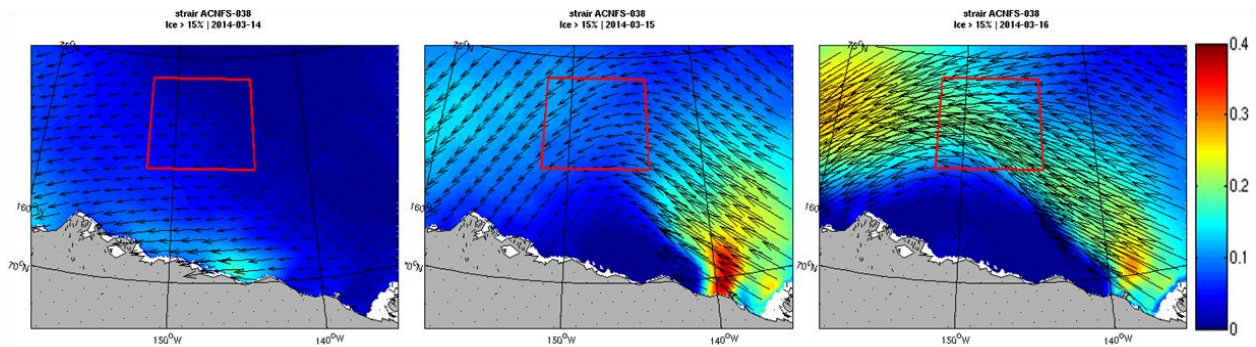


Figure 23: Beaufort Sea ACNFS Air stress for March 14, 15, and 16, 2014. ICEX 2014 ice camp general region outlined in red.

Figure 24 depicts a MODIS and RADARSAT-2 mosaic image for March 16th, 2014. Fracturing is seen throughout the region with fractures running from northwest to southeast and from north to south. The strong fracturing was predicted as early as in the ACNFS 48 hour forecast, as seen in Figure 25.

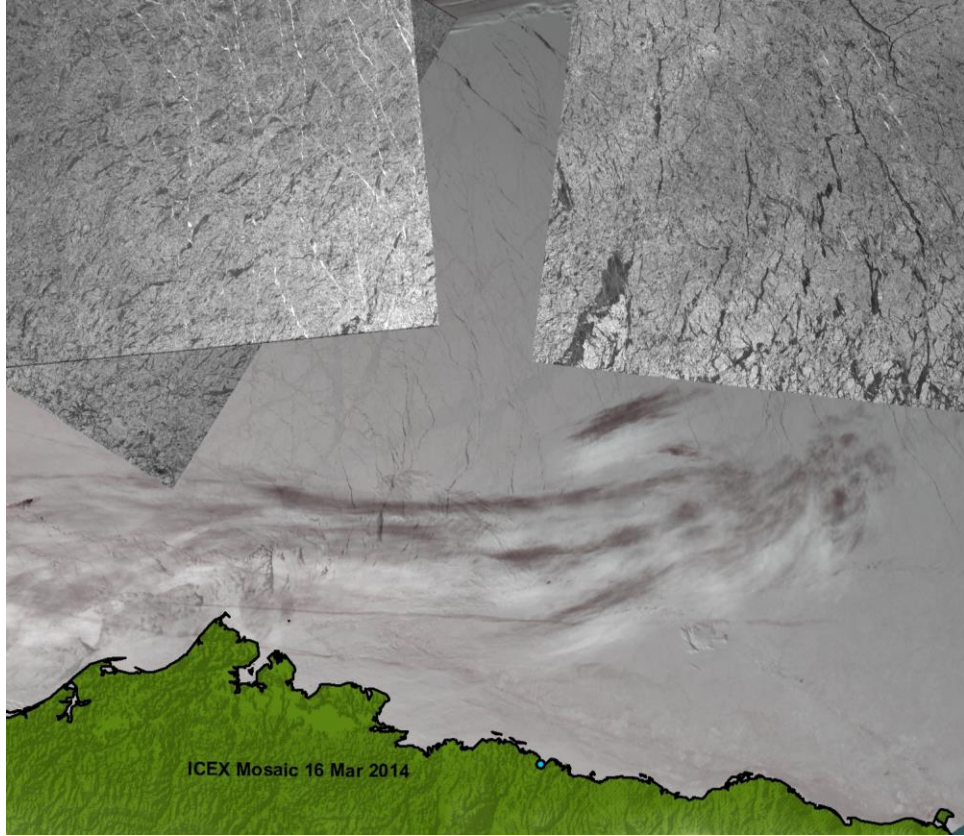


Figure 24: Beaufort Sea MODIS and RADARSAT-2 mosaic image for March 16, 2014.

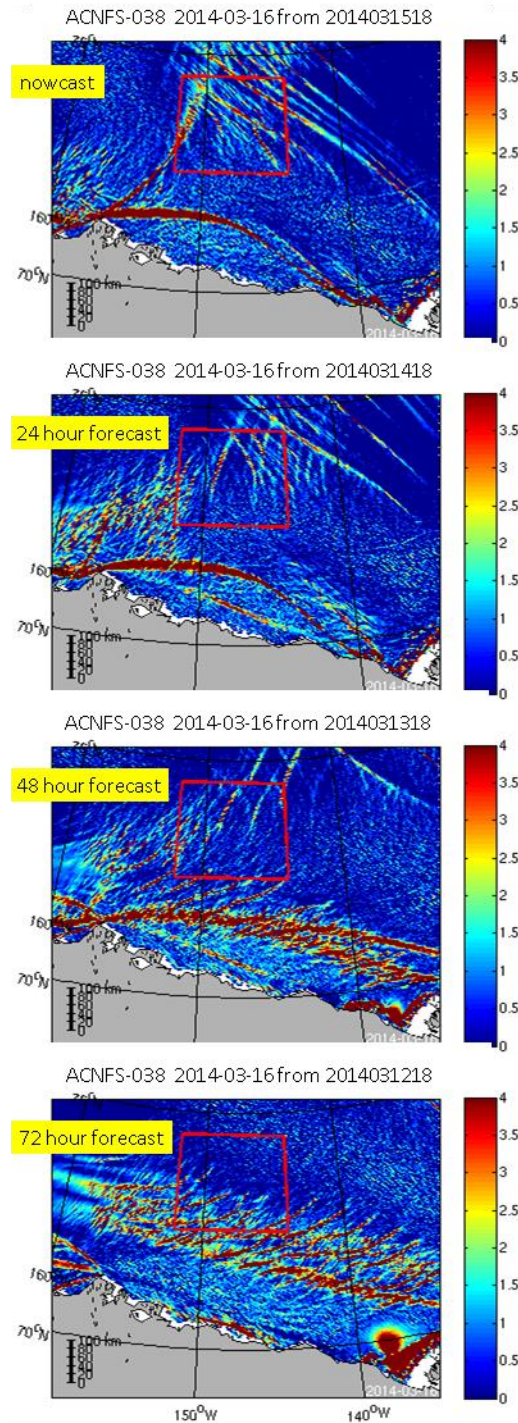


Figure 25: Beaufort Sea ACNFS Opening rate nowcast and forecasts for March 16, 2014.

The strong reversal of forcing and ice velocity occurred March 20th to March 21st and was predicted by ACNFS/NAVGEN as early as the 6-day forecast as shown in Figure 26.

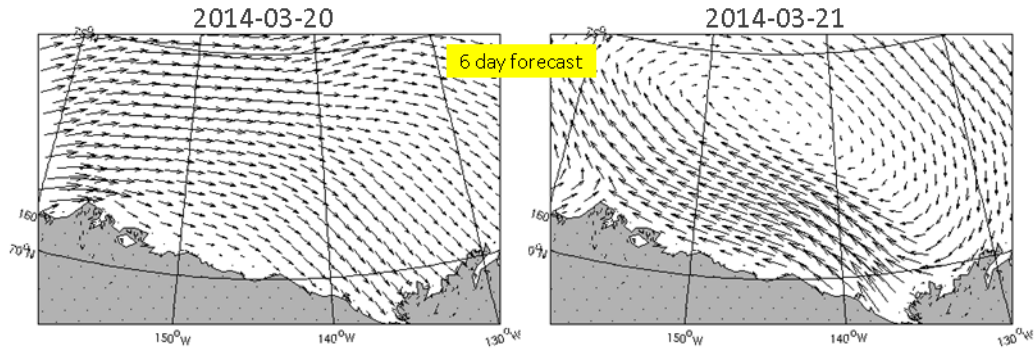


Figure 26: Beaufort Sea ACNFS Ice velocity 6-day out forecast for March 20, 2014.

Some central Beaufort openings occurred on the 20th and 21st, but strong north south fracturing occurred on the 22nd. The openings on March 22nd were forecasted in the 24 hour forecast as shown in Figure 27. Figure 28 shows a MODIS mosaic showing the fractures on the 22nd as well as wind and ice drift vectors.

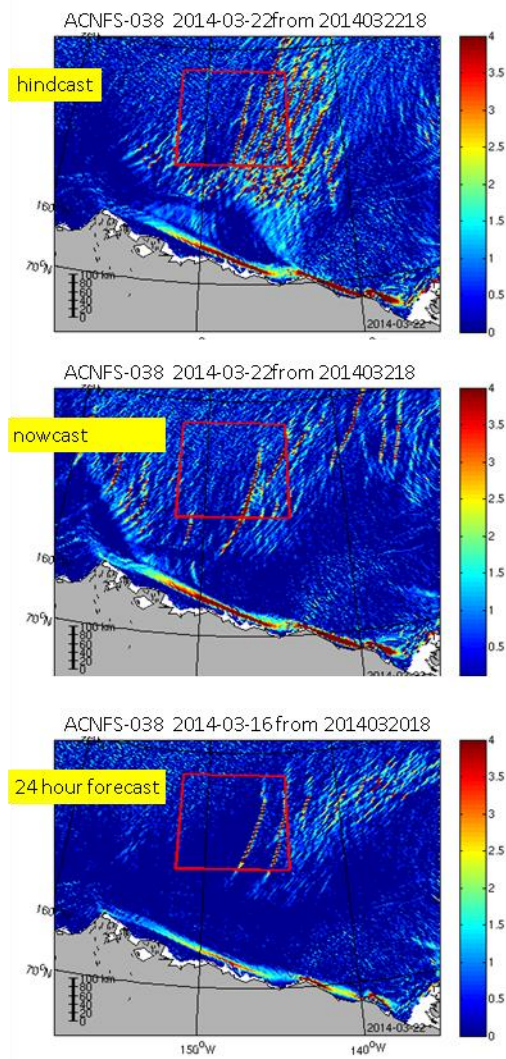


Figure 27: Beaufort Sea ACNFS Opening rate hindcast, nowcast, and 24-hour forecast.

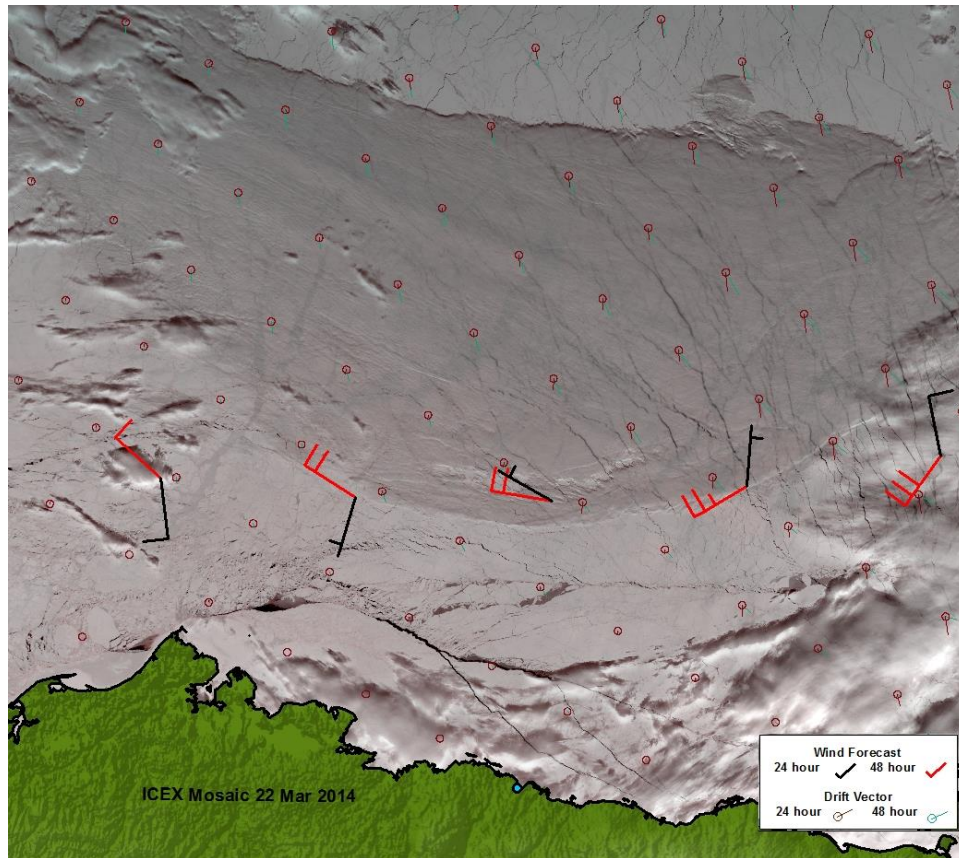


Figure 28: Beaufort Sea MODIS mosaic image for March 22, 2014. Wind and ice drift vectors overlaid.

3.4 Polynyas

ACNFS does an excellent job capturing polynyas. In the opening rate plots, polynyas are well depicted and are often differentiated from fracture areas with sharper delineation from the surrounding ice, but they are most reliably seen with the ice concentration. Polynyas are persistent large non-linear shaped regions of open water with length scales on the order of 100km and generally much larger area than ice fractures and leads (Martin, 2001). With their persistence and size, they are typically captured in satellite ice concentration imagery and consequently the model ice concentration output. There are two types of polynyas: coastal and open ocean. Coastal polynyas are found adjacent to coastlines and are driven by persistent offshore winds. Open ocean polynyas are enclosed in the pack ice and are driven by warm water upwelling.

Figure 29 shows an example of an open water polynya seen in MODIS imagery and ACNFS opening rate, and ACNFS concentration. This particular polynya persisted for over a month until consumed by the ice edge.

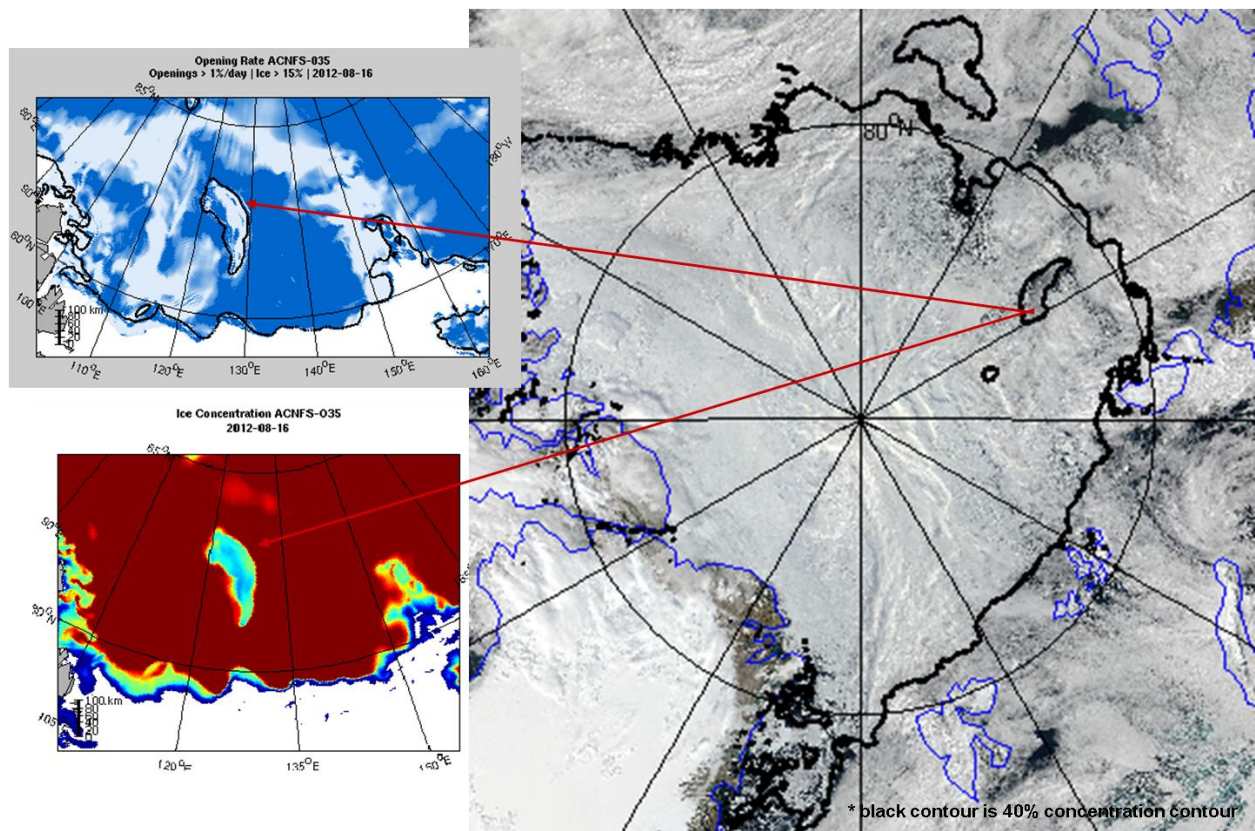


Figure 29: Open ocean polynya August 16, 2012. Right: MODIS imagery (NASA, 2014) with ACNFS 40% concentration contour overlaid in black. Top, left: ACNFS opening rate with 40% concentration contour. Bottom, left: ACNFS ice concentration.

Figure 30 and Figure 31 illustrate an example of coastal polynyas and the ACNFS forecasting capability. Figure 30 shows 8 consecutive days of VIIRS near-constant contrast (NCC) imagery over the Kara Sea starting April 15, 2014. Note the polynyas in the south Kara Sea on either side of the Kara Strait. The polynyas fluctuate in size as the ice moves away and towards the shores.

Figure 31 shows the nowcast and 7-day opening rate forecasts from April 15, 2014. The 70% ice concentration for each model forecast is contoured and overlaid in black. Starting from the nowcast – day April 15, two polynya can be seen, one on each side of the Kara Strait. The polynya on the east side persists throughout the time period increasing and decreasing slightly in size. The polynya on the west side shrinks and then returns and extends northward along the east Novaya Zemlya coastline. These same features are seen in the ACNFS model output.

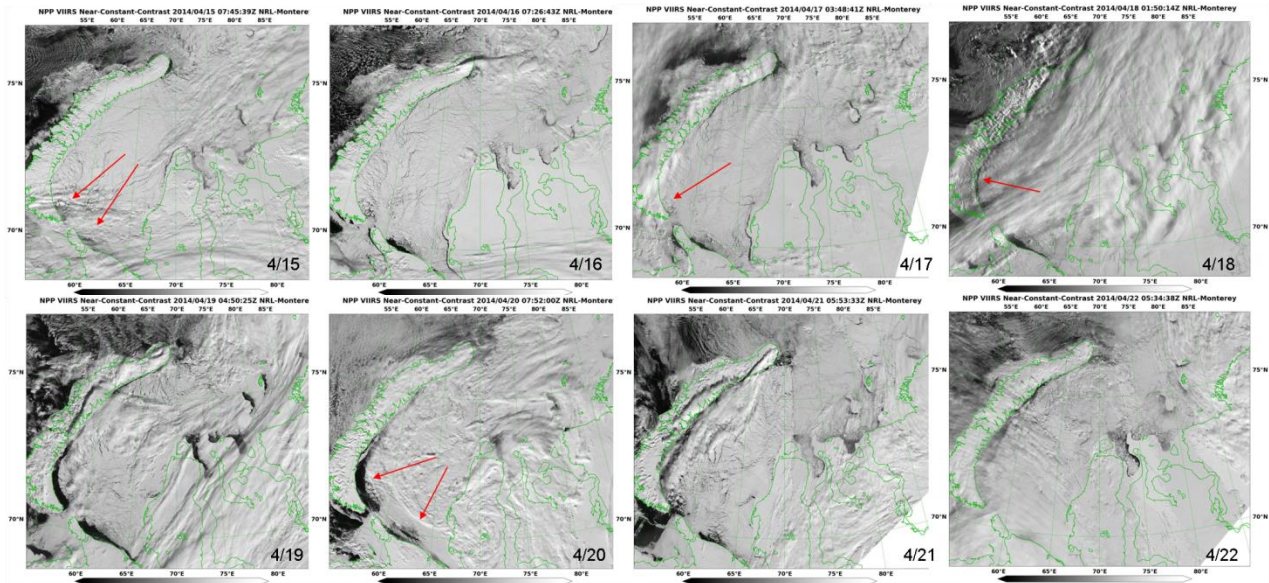


Figure 30: VIIRS Near-Constant Contrast (NCC) imagery (NRL-MRY, 2014) over Kara Sea from April 15 through April 22, 2014.

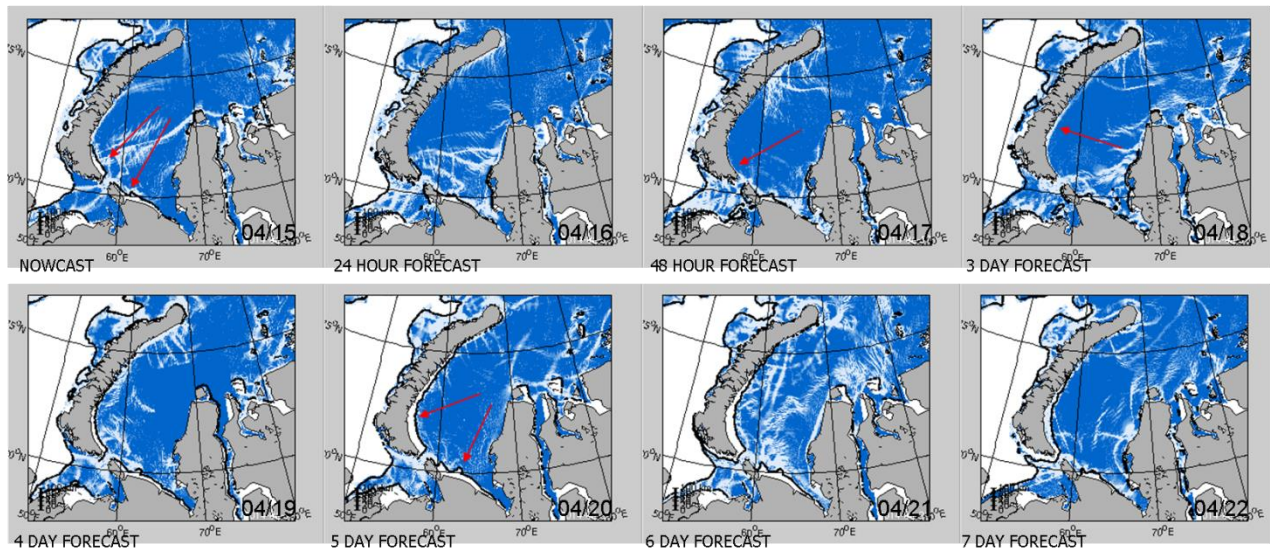


Figure 31: ACNFS Opening rate with 70% ice concentration contour in black for Kara Sea from April 15 through April 22, 2014.

3.5 Seasonal Variation

Seasonal variability in the performance of opening rate forecasts is seen in the magnitudes of the RMS error and classification errors sensitivity and specificity. Figures 33 and 34 show the seasonal/monthly variability. Forecasting is more reliable in the winter than in the spring, but at the same time is slightly less likely to predict non-openings, but slightly more likely to predict openings. The accuracy remains consistent between seasons. Forecast specificities were lower in February/March as the number of ice cells reaches a maximum. (Figure 34)

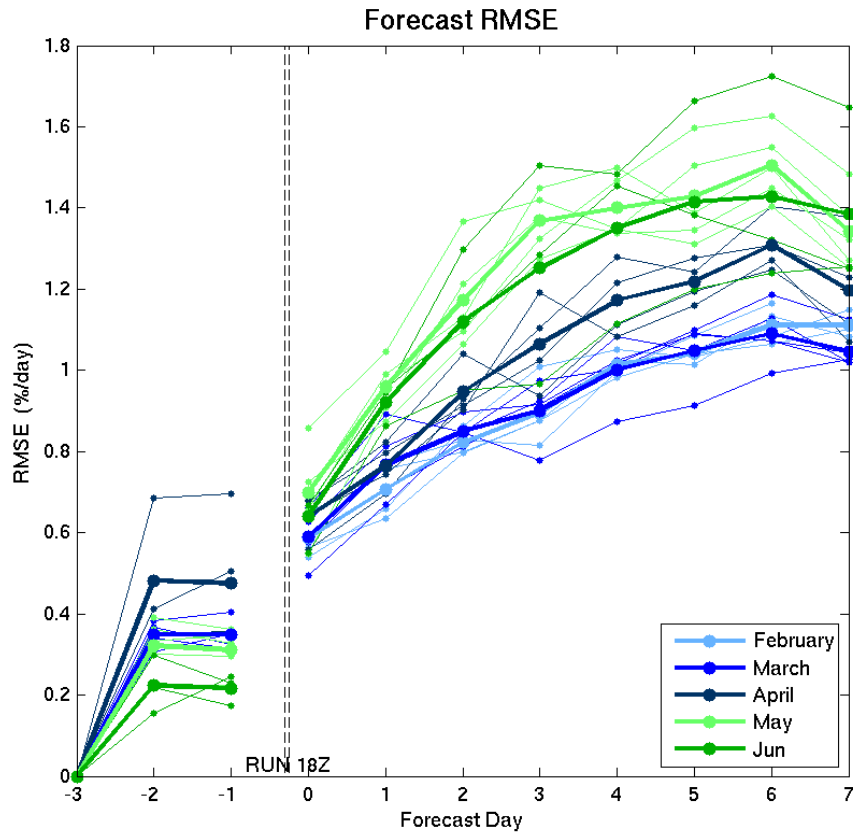


Figure 32: RMS Error of the opening rate forecasts. Winter months are shown in shades of blue. Spring months are shown in shades of green.

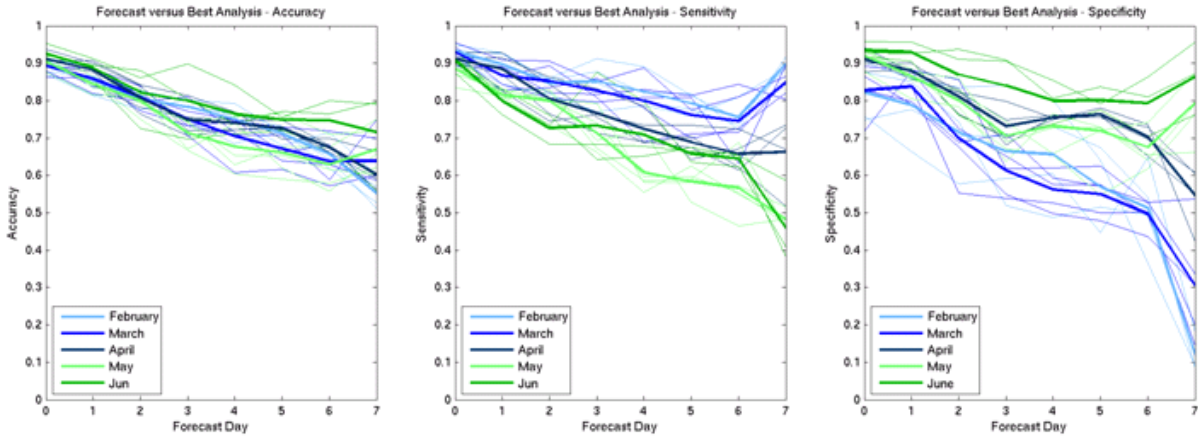


Figure 33: Specificity, Sensitivity, and Accuracy classification errors of opening rate forecasts. Winter months are shown in shades of blue. Spring months are shown in shades of green.

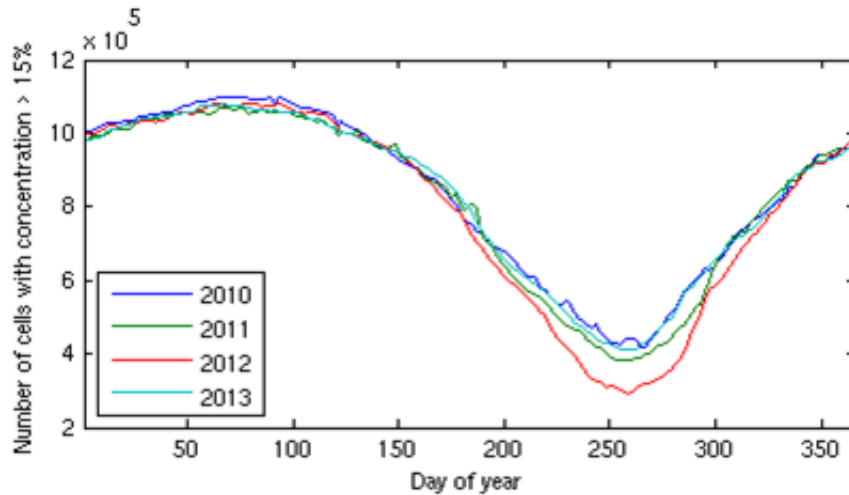


Figure 34: Daily number of ice cells with concentration greater than 15%.

The overall accuracy shows little difference between the seasons, but the sensitivity and specificity show changes especially after 72 hours. In winter, when there are fewer ice openings, ACNFS does a better job predicting the opening regions, whereas in the spring as more fracturing occurs, the model does a better job predicting the non-openings.

Table 1 of Section 3.2.1 listed the category totals from all of the FLAP message comparisons. Table 3 lists the same category totals from all the FLAP message comparisons against ACNFS by season/month. As with the model forecast to model hindcast comparisons, winter had overall better results than spring in predicting the openings.

Winter: Jan – Mar	Fracture Regions			Percent of Fracture Regions								
	✓	?	X	✓	?				?	✓ + ?	X	
					off-set	partial	subset	weak				
ACNFS	2	7	0	22%	11%	11%	56%	0%	78%	100%	0%	
GOFS	3	6	0	33%	22%	11%	33%	0%	67%	100%	0%	
ACNFS - Accumulated	4	5	0	44%	11%	0%	44%	0%	56%	100%	0%	

Spring: Apr – Jun	Fracture Regions			Percent of Fracture Regions								
	✓	?	X	✓	?				?	✓ + ?	X	
					off-set	partial	subset	weak				
ACNFS	15	23	9	32%	6%	17%	15%	11%	49%	81%	19%	
GOFS	13	24	12	27%	2%	14%	18%	14%	49%	76%	24%	
ACNFS - Accumulated	16	31	1	33%	2%	8%	50%	4%	65%	98%	2%	

Summer: Jul – Sep	Fracture Regions			Percent of Fracture Regions								
	✓	?	X	✓	?				?	✓ + ?	X	
					off-set	partial	subset	weak				
ACNFS	6	17	3	23%	8%	42%	15%	0%	65%	88%	12%	
GOFS	4	14	11	14%	0%	34%	14%	0%	48%	62%	38%	
ACNFS - Accumulated	9	15	3	33%	0%	26%	30%	0%	56%	89%	11%	

Fall: Oct – Dec	Fracture Regions			Percent of Fracture Regions								
	✓	?	X	✓	?				?	✓ + ?	X	
					off-set	partial	subset	weak				
ACNFS	26	42	5	35%	3%	18%	24%	12%	57%	92%	8%	
GOFS	22	41	10	30%	5%	21%	18%	12%	56%	86%	14%	
ACNFS - Accumulated	38	44	2	45%	4%	7%	37%	5%	52%	97%	2%	

Table 3: FLAP area prediction comparison categories totals broken out by season.

4 Summary and Recommendations

This validation assessment was performed using ACNFS with some limited comparisons with GOFS 3.1. Results of the validation testing of the ACNFS’ best quality prediction against actual FLAP messages as ground truth and model forecasts against reference hindcasts were presented. Additional comparisons were shown from ICEX-2014 and isolated available imagery. Table 4 presents the summary statistics for the NIC FLAP area comparisons. The FLAP areas were strongly matched in the ACNFS accumulated openings at 40%, while only 4% were missed completely. Table 5 presents the summary statistics for the FLAP forecast capability as compared with persistence for the first 72 hours of forecasts. The ACNFS forecast showed a 47% improvement over persistence for the nowcast in terms of RMSE error with an 18% improvement out to 3 days. Accuracy, sensitivity, and specificity forecast improvements were approximately 30% for the nowcast and 20% for the 3 day forecast.

	Percent of FLAP Message Fracture Regions			
	Strong match	Partial match	Strong and Partial match	No match
ACNFS accumulated openings	40%	57%	97%	4%

Table 4: FLAP area skill totals.

	Nowcast	24 hour	48 hour	72 hour
RMSE ACNFS	0.63	0.82	0.98	1.09
RMSE Persistence	1.19	1.28	1.3	1.33
Accuracy ACNFS	0.9	0.86	0.81	0.75
Accuracy Persistence	0.7	0.64	0.62	0.62
Sensitivity ACNFS	0.91	0.85	0.81	0.78
Sensitivity Persistence	0.73	0.67	0.64	0.64
Specificity ACNFS	0.88	0.86	0.77	0.7
Specificity Persistence	0.65	0.6	0.57	0.58

Table 5: Flap area forecast skill metrics for first 72 hours.

Overall, ACNFS provided a reasonable prediction of the openings not available elsewhere in either nowcast or forecast mode and performed better than simple persistence of the best model hindcast. This validation has shown that ACNFS and GOFS 3.1 nowcast/forecasts provide an indication of fracture regions.

Therefore, it is recommended for the National Ice Center to utilize ACNFS (and GOFS 3.1, when available) opening rate nowcasts/forecasts in conjunction with available imagery to better describe a current realistic sea ice scene in exercise/operations planning for the Navy.

5 Acknowledgements

This work was funded as part of the NRL 6.4 Ice Modeling Assimilation from Satellites project, managed by the Space and Naval Warfare Systems Command under program element 0603207N. The numerical hindcasts and forecasts were performed on the Navy DSRC iDataPlex computers (Kilrain and Haise) at Stennis Space Center, Mississippi using grants of computer time from the DoD High Performance Computing Modernization Program. The Validation test Panel consisted of Chris DeHaan (NAVOCEANO), Behn Zib (National Ice Center), Jenny Hutchings (Oregon State University), Pam Posey (Naval Research Laboratory) and Julie Crout (Vencore). This is NRL contribution NRL/MR/7320-15-9590, which is approved for public release and distribution is unlimited.

6 References

- Cummings, J.A. and O.M. Smedstad, 2013. Variational data assimilation for the global ocean. In *Data Assimilation for Atmospheric, Oceanic and Hydrologic Applications (Vol. II)*. S.K. Park and L.Xu, eds, Springer-Verlag, Berlin, Heidelberg, http://dx.dio.org/10.1007/978-3-642-35088-7_13.
- Helfrich, S., 2012: Operational Evaluation Report for the Arctic Cap Nowcast/Forecast System (ACNFS), Naval Ice Center (NAVICEN), 38 pp.
- Hogan, T.F., T.E. Rosmond, and R. Gelaro, 1991: The description of the Navy Operational Global Atmospheric Prediction System's Forecast model (NOGAPS), NOARL Report 13, Naval Research Laboratory, Stennis Space Center, MS.
- Hunke, E.C. and W. H. Lipscomb, 2004: CICE: The Los Alamos Sea Ice Model, documentation and software, version 3.1, LA-CC-98-16, Los Alamos Natl. Lab., Los Alamos, NM, 56 pp.
- Lipscomb, W.H., E.C. Hunke, W. Maslowski, and J. Jakacki, 2007: Ridging, strength, and stability in high-resolution sea ice models, *Journal of Geophysical Research*, 112, C03S91, pp. 1848-1865.
- Lindsay, R.W. and H.L. Stern, 2003: The RADARSAT Geophysical Processor System: Quality of Sea Ice Trajectory and Deformation Estimates. *Journal of Oceanic and Atmospheric Technology*, 20 1333-1347.
- Martin, S., 2001: Polynyas. In *Encyclopedia of Ocean Sciences*, ed. Steele, J.H., Turekian, K.K., Thorpe, S.A., Vol. 3, pp. 2241-2247. London, Academic Press, 7pp.
- Metzger, E.J., P.G. Posey, P. Thoppil, T.L. Townsend, A.J. Wallcraft, O.M. Smedstad, D.S. Franklin, L. Zamudio, and M.W. Phelps, 2014: Validation Test Report for the Global Ocean Forecast System 3.1 -1/12° HYCOM/NCODA/CICE/ISOP. NRL Memo. Report, NRL/MR/7320-14-xxxx.
- Metzger, E.J., A.J. Wallcraft, P.G. Posey, O.M. Smedstad, and D.S. Franklin, 2013: The Switchover from NOGAPS to NAVGEM 1.1 Atmospheric Forcing in GOFS and ACNFS. NRL/MR/7320—13,9486, Naval Research Laboratory, Stennis Space Center, MS, 13 pp.
- Metzger, E.J., O.M. Smedstad, P. Thoppil, H.E. Hurlburt, D.S. Franklin, G. Peggion, J.F. Shriver T.L. Townsend and A.J. Wallcraft, 2010: Validation Test Report for the Global Ocean Forecast System V3.0 -1/12° HYCOM/NCODA: Phase II. NRL Memo. Report, NRL/MR/7320--10-9236.
- NASA Earth Observing System Data and Information System, Rapid Response, 2014: MODIS Aqua Arctic mosaic imagery.
- Naval Research Laboratory – Monterey, 2014: VIIRS Imagery.
- Posey, P.G., E.J. Metzger, A.J. Wallcraft, R.H. Preller, O.M. Smedstad, M.W. Phelps, 2010: Validation of the 1/12° Arctic Cap Nowcast/Forecast System (ACNFS). NRL/MR/7320—10-9287, Naval Research Laboratory, Stennis Space Center, MS, 55 pp.
- Thorndike, A.S., D.A. Rothrock, G.A. Maykut, and R. Colony, 1975: The thickness distribution of sea ice. *Journal of Geophysical Research*, 80, pp. 4501-4513.

7 Acronyms

ACNFS	Arctic Cap Nowcast/Forecast System
CICE	Community Ice Code
COMSUBFOR	Commander, Submarine Forces
DoD	Department of Defense
EVP	Elastic Viscous Plastic
FLAP	Fractures/Leads and Polynyas
GOFS	Global Ocean Forecast System
HYCOM	HYbrid Coordinate Ocean Model
ICEX	Ice Exercise
MODIS	Moderate Resolution Imaging Spectroradiometer
NAVGENM	NAVy Global Environmental Model (NAVGENM)
NAVICECEN	Naval Ice Center
NAVOCEANO	Naval Oceanographic Office
NCODA	Navy Coupled Ocean Data Assimilation
NIC	National Ice Center
NOGAPS	Navy Operational Global Atmospheric Prediction System
NRL	Naval Research Laboratory
OPEVAL	Operational Evaluation (OPEVAL)
RGPS	RADARSAT Geophysical Processor System
RMSE	Root Mean Square Error
SSMIS	Special Sensor Microwave Imager/Sounder